ELSEVIER

Advances in Colloid and Interface Science 123–126 (2006) 259–293

ADVANCES IN COLLOID AND INTERFACE SCIENCE

www.elsevier.com/locate/cis

Coalescence stability of emulsions containing globular milk proteins

Slavka Tcholakova [a], Nikolai D. Denkov [a], Ivan B. Ivanov [a,*], Bruce Campbell [b]

[a] *Laboratory of Chemical Physics and Engineering, Faculty of Chemistry, Sofia University, 1 James Bourchier Avenue, 1164 Sofia, Bulgaria*
[b] *Kraft Foods Global Inc., 801 Waukegan Road, Glenview, Illinois 60025, USA*

Available online 18 July 2006

Abstract

This review summarizes a large set of related experimental results about protein adsorption and drop coalescence in emulsions, stabilized by globular milk proteins, β-lactoglobulin (BLG) or whey protein concentrate (WPC). First, we consider the effect of drop coalescence on the mean drop size, d_{32}, during emulsification. Two regimes of emulsification, surfactant-rich (negligible drop coalescence) and surfactant-poor (significant drop coalescence) are observed in all systems studied. In the surfactant-rich regime, d_{32} does not depend on emulsifier concentration and is determined mainly by the interfacial tension and the power dissipation density in the emulsification chamber, ε. In the surfactant-poor regime and suppressed electrostatic repulsion, d_{32} is a linear function of the inverse initial emulsifier concentration, $1/C_{INI}$, which allows one to determine the threshold emulsifier adsorption needed to stabilize the oil drops during emulsification, Γ^* (the latter depends neither on oil volume fraction nor on ε). Second, we study how the BLG adsorption on drop surface changes while varying the protein and electrolyte concentrations, and pH of the aqueous phase. At low electrolyte concentrations, the protein adsorbs in a monolayer. If the pH is away from the isoelectric point (IEP), the electrostatic repulsion keeps the adsorbed BLG molecules separated from each other, which precludes the formation of strong intermolecular bonds during shelf-storage as well as after heating of the emulsion. At higher electrolyte concentration, the adsorption Γ increases, as a result of suppressed electrostatic repulsion between the protein molecules; monolayer or multilayer is formed, depending on protein concentration and pH. The adsorption passes through a maximum (around the protein IEP) as a function of pH. Third, the effect of various factors on the coalescence stability of "fresh" emulsions (up to several hours after preparation) was studied. Important conclusion from this part of the study is the establishment of three different cases of emulsion stabilization: (1) electrostatically-stabilized emulsions with monolayer adsorption, whose stability is described by the DLVO theory; (2) emulsions stabilized by steric repulsion, created by protein adsorption multilayers — a simple model was adapted to describe the stability of these emulsions; and (3) emulsions stabilized by steric repulsion, created by adsorption monolayers. Fourth, we studied how the emulsion stability changes with storage time and after heating. At high electrolyte concentrations, we find a significant decrease of the coalescence stability of BLG-emulsions after one day of shelf-storage (aging effect). The results suggest that aging is related to conformational changes in the protein adsorption layer, which lead to formation of extensive lateral non-covalent bonds (H-bonds and hydrophobic interactions) between the adsorbed molecules. The heating of BLG emulsions at high electrolyte concentration leads to strong increase of emulsion stability and to disappearance of the aging effect, which is explained by the formation of disulfide bonds between the adsorbed molecules. The emulsion heating at low electrolyte concentration does not affect emulsion stability — this result is explained with the electrostatic repulsion between the adsorbed molecules, which keeps them separated so that no intermolecular disulfide bonds are formed. Parallel experiments with WPC-stabilized emulsions show that these emulsions are less sensitive to variations of pH and thermal treatment; no aging effect is detected up to 30 days of storage. The observed differences between BLG and WPC are explained with the different procedures of preparation of these protein samples (freeze-drying and thermally enhanced spray-drying, respectively). Our data for emulsion coalescence stability are compared with literature results about the flocculation stability of BLG emulsions, and the observed similarities/differences are explained by considering the structure of the protein adsorption layers.

Keywords: Protein stabilized emulsions; Coalescence stability of emulsions; Protein adsorption; Emulsification; Osmotic pressure of emulsions; β-lactoglobulin; Whey protein

* Corresponding author. Tel.: +359 2 962 5310; fax: +359 2 962 5643.
E-mail address: II@lcpe.uni-sofia.bg (I.B. Ivanov).

0001-8686/$ - see front matter © 2006 Elsevier B.V. All rights reserved.
doi:10.1016/j.cis.2006.05.021

Contents

1. Introduction

Proteins are widely used as emulsion stabilizers in food industry [1–3]. Similarly to the conventional surfactants, proteins facilitate the breakage of oil drops during emulsification (by lowering the oil–water interfacial tension), and stabilize the drops against coalescence during emulsification [4–8] as well as upon subsequent storage of the formed emulsions [1–3].

The efficiency of protein emulsifiers depends strongly on the density and structure of the protein adsorption layers on the drop surface. For this reason, numerous experimental and theoretical studies were performed to clarify the role of various factors on protein adsorption [9–21]. In general, the adsorption process of protein molecules is known to consist of at least two stages: (1) transport and attachment of the molecules to the interface; (2) structural rearrangement of the adsorbed molecules with possible partial unfolding and formation of intermolecular bonds [9–15,21]. The time scale of the second stage could be rather slow (from seconds to months), which may lead to very complex evolution of the protein adsorption layers and the respective emulsions properties (e.g., upon shelf-storage). The amount of adsorbed protein, the kinetics of adsorption, and the structure of the formed layers depend on many factors, such as protein and electrolyte concentration, pH, pre-heating of the protein solutions, type of apolar phase, etc., whose effects are still not well understood and deserve further studies.

Emulsions are thermodynamically unstable and various processes lead to changes in the drop size-distribution and/or emulsion structure. The most common processes of emulsion destabilization are drop-drop coalescence, flocculation, creaming, and the Ostwald ripening. During flocculation and creaming, the emulsion structure changes, while drop-size distribution may remain unaltered. In contrast, the drop-drop coalescence and the Ostwald ripening lead to changes in the drop-size distribution with time.

The main focus of the current review is the coalescence stability of oil-in-water emulsions, stabilized by globular proteins, whereas for the other modes of emulsion destabilization we refer to the literature. Reviews on the role of various factors on the flocculation stability of emulsions containing globular proteins are presented in Refs. [2,22]. In Section 12 below we summarize some of the important results from these studies and compare the flocculation stability with our results for the emulsion coalescence stability. The drop flocculation affects strongly the creaming stability of emulsions, and this relation is analyzed and discussed in Refs. [23–26]. The Ostwald ripening is usually negligible for protein-stabilized triglyceride-in-water emulsions, which are the main subject of the current review — therefore, this mode of emulsion destabilization will not be discussed here.

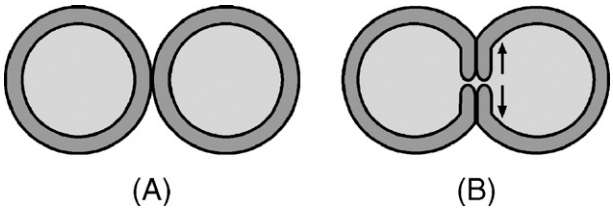

Fig. 1. Schematic presentation of the mechanism of drop coalescence after mechanical rupture of protective protein layers. (A) Spherical drops, covered with protein layers of certain mechanical strength. The protein layers on two neighboring drops can touch each other, if no long-ranged repulsion between the drop surfaces is present; (B) during drop deformation, caused by compression of the drops against each other or during emulsion shear, the drop surface expands and the protective protein layer can rupture, creating unprotected zones in the emulsion film.

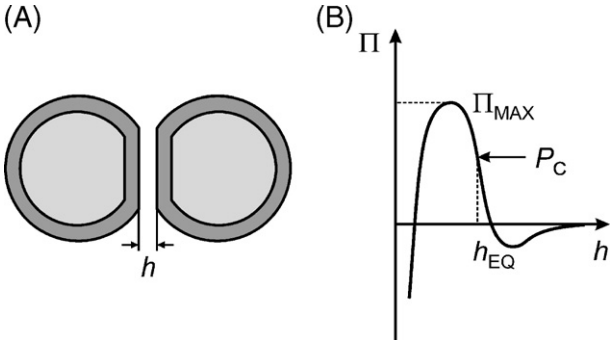

Fig. 2. Schematic presentation of the barrier created by surface forces, which protects the drops against coalescence. (A) Without strong compression, the drop surfaces cannot come in direct contact with each other due to the presence of long-ranged electrostatic or steric repulsion; (B) schematic presentation of the disjoining pressure isotherm, $\Pi(h)$, with barrier Π_{MAX}, according to the DLVO theory. This barrier can be overcome only if the capillary pressure, P_C, compressing the surfaces against each other is higher than Π_{MAX}; if $P_C < \Pi_{MAX}$, an equilibrium film with thickness h_{EQ} is formed.

Drop coalescence is a process in which two drops merge to form a larger drop. The protein adsorption layers may prevent this process, by stabilizing the emulsion films formed between neighboring drops against rupture. The detailed molecular mechanisms for emulsion stabilization by adsorbed proteins are still poorly understood and are under discussion [23,27,28]. In the literature, the ability of protein molecules to stabilize emulsion films is attributed to: (1) formation of adsorption layers with certain mechanical stability in the plane of the layers, which protect the film against rupture [2,28] (see Fig. 1); or (2) creating a barrier in the disjoining pressure, Π (force per unit area of the film), which opposes film thinning and, thus, prevents direct contact of the two opposite film surfaces (Fig. 2).

It is usually assumed that the rheological properties of the adsorption layers are of primary importance for the first type of protein stabilization (formation of mechanically stable adsorption layers) [2,28–35]. In the frame of this reasoning, Graham and Phillips [29,30] reported certain correlation between the rheological properties of the protein adsorption layers (dilatation and shear elasticity) and foam stability. However, the same authors did not find direct correlation between emulsion stability and the rheological properties of the respective adsorption layers [29,30]. The absence of such correlation was found also in a recent study [36], which showed that the aging (shelf-storage at room temperature) and the heating of β-lactoglobulin (BLG) stabilized emulsions lead to opposite effects on emulsion coalescence stability — the aging decreases, whereas the heating increases the stability, although both treatments are known to increase the elasticity of BLG adsorption layers [35]. These examples evidence that the relationship between the visco-elastic

properties of protein adsorption layers and emulsion stability is not straightforward.

In other studies [37–39], the stabilizing role of the adsorbed protein molecules is explained by their effect on the surface forces, e.g., by modifying the electrical potential of the drop surface [37–39] and the van der Waals interactions [40,41], or by creating a steric barrier to drop-drop coalescence [38,39,42,43]. The comparison between the experimental results and the theoretical estimates showed that the emulsion stability could be described by the DLVO-theory for some systems. For example, Graham and Phillips [29,30] showed that the electrostatic interactions were important away from the IEP. In a more recent study, Narsimhan [38] showed that the steric repulsion between the protein adsorption layers should also be taken into account to explain the emulsion stability, along with the DLVO interactions.

The major aims of the current review are to summarize our recent results [7,8,36,39,40,44–47] about the effects of various factors (protein concentration and adsorption, drop size, electrolyte concentration, pH, thermal treatment and time of shelf-storage) on the coalescence stability of BLG-containing emulsions, and on this basis, to discuss and clarify whenever possible the mechanisms of stabilization by the protein adsorption layers. To achieve these aims, we combined several experimental methods, which provide complementary information about the effects of the various factors on protein adsorption and on emulsion coalescence stability. All studies were performed with batch emulsions to avoid (often questionable) transfer of conclusions from model experiments with single air–water or oil–water interface to the real emulsions. The results obtained allowed us to make several conclusions about the modes of emulsion stabilization by BLG, which are probably relevant to emulsions stabilized by other globular proteins, as well.

The review is structured as follows. In Section 2 we describe the materials and experimental methods used. In Section 3 we summarize the main results regarding the role of drop-drop coalescence in the emulsification process. In Section 4 we present results clarifying how the drop size affects the emulsion coalescence stability. In Section 5 we describe new experimental procedure for determination of the dependence of the emulsion osmotic pressure (used in our studies to characterize the emulsion coalescence stability) on the oil volume fraction. In Sections 6 and 7 we present the experimental results about the effects of protein concentration, pH, and electrolyte concentration on protein adsorption and emulsion coalescence stability. These results are combined in Section 8 to describe three different modes of emulsion stabilization and to propose respective theoretical interpretation of the data. In Section 9 we present results about the effects of heating and storage time on coalescence stability, and explain these results by considering the changes in the protein adsorption layers. In Section 10 we compare the properties of BLG and whey protein concentrate of technical grade (WPC) as emulsifiers and explain qualitatively the observed differences. The possible mechanisms of emulsion film rupture are discussed in Section 11. In Section 12, we compare our results for the coalescence stability with literature results about the flocculation stability of BLG emulsions. The main results and conclusions are summarized in Section 13. The list of the used abbreviations and the notation is presented in Section 14.

2. Materials and methods

2.1. Materials

As globular milk protein we studied β-lactoglobulin (BLG) from bovine milk, as received from Sigma (Cat. # L-0130, Lot # 052K7018 for the results shown in Sections 6.2, 6.3, 7.2, 7.3, 9.2 and Lot No. 124H7045 for the results described in Sections 6.1, 7.1, 9.1 [48,49]). Whey protein concentrate of technical-grade, WPC (trade name AMP 8000; product of Proliant Inc., Ankeny, IA, USA) was used as emulsifier, which contains 71.7 wt.% globular proteins (44% of which is β-lactoglobulin as the main component), 17.2 wt.% carbohydrates, 6.2 wt.% water, 2.8 wt.% ash, and 2.1 wt.% fat.

In several series of emulsification experiments, low molecular mass surfactants were also used for comparison with proteins: the anionic sodium dodecyl sulfate (SDS; product of Acros) and the nonionic hexadecylpolyoxyethylene-20 (Brij 58; product of Sigma).

Commercial grade soybean oil (SBO) was used as the oil phase. In the experiments aimed to study coalescence stability, SBO was purified from polar contaminants by multiple passes through a glass column, filled with Florisil® adsorbent (Sigma) [50]. The interfacial tension of the purified SBO was $\sigma_{OW}=29.5\pm 0.5$ mN/m. In the emulsification experiments, commercial SBO was used without additional purification ($\sigma_{OW}=27\pm1$ mN/m). Comparative emulsification experiments with purified and non-purified SBOs gave similar results, so that oil purification was not needed for these experiments.

The protein solutions were prepared with deionized water, purified by Milli-Q Organex system (Millipore), and always contained 0.01 wt.% of the antibacterial agent NaN_3 (Riedel-de Haën). The ionic strength was adjusted between 1.5 mM (only NaN_3) and 1 M, by using NaCl. The desired pH value was achieved by addition of small aliquots of 0.1 M NaOH or 0.1 M HCl into the BLG solutions, whereas 1.1 M lactic acid was used for pH reduction of the WPC solutions.

2.2. Emulsion preparation

Two different emulsification procedures were used, depending on the specific aim:

(1) In the experiments aimed to study the dependence of emulsion coalescence stability on the factors related to system composition (such as protein and electrolyte concentrations, pH, aging time and heating), the emulsions were prepared by an Ultra-Turrax T25 rotor-stator homogenizer (Janke & Kunkel GmbH & Co., IKA-Labortechnik, Staufen, Germany). This homogenizer gave emulsions with similar drop-size distributions, which allowed us to separate the effect of drop size from the other effects [36,39,45]. The emulsification procedure consisted of intense stirring of 35 mL protein

solution and 15 mL soybean oil for 3 min at 13,500 rpm, so that 30 vol.% oil-in-water emulsion with mean volume-surface drop radius $R_{32} \approx 20$ μm was formed.

(2) In the experiments aimed to clarify the effects of various factors on the mean drop size during emulsification, we used the narrow-gap homogenizer and two-step procedure [7,8]. First, an oil-in-water premix was prepared by hand-shaking a vessel containing 200 mL oil and 520 mL aqueous phase (28 vol.% oil). In the second step, this premix was circulated for 10 min in a closed loop through the homogenizer to achieve steady-state drop-size distribution. The intensity of mixing was controlled by varying the applied pressure at the homogenizer inlet and was characterized by the power dissipation density in the homogenizer head, ε [J/s kg] (see Ref. [7] for more detailed description).

2.3. Determination of mean drop size

The drop-size distribution in the studied emulsions was determined by video-enhanced optical microscopy [51–53]. Specimens for analysis were taken immediately after emulsion preparation to avoid possible artifacts related to emulsion creaming or drop coalescence after emulsification [53]. The oil drops were observed with an optical microscope, connected to a CCD camera and a video-recorder. The drop diameters were measured from the recorded video-frames, using custom-made image analysis software. The diameters of at least 10,000 drops in 2 to 5 independently prepared emulsions were measured for each system. The mean volume-surface diameter, d_{32}, was calculated from the relation:

$$d_{32} = \frac{\sum_i N_i d_i^3}{\sum_i N_i d_i^2} \quad (1)$$

where N_i is the measured number of drops with diameter d_i.

2.4. Determination of protein adsorption

The protein adsorption on the surface of the emulsion drops, Γ, was determined from the decrease of protein concentration in the aqueous phase, $\Delta C = C_{INI} - C_{SER}$, as a result of the emulsification process [36,39,45,47]. Here C_{INI} is the initial protein concentration in the aqueous solution before emulsification, while C_{SER} is the concentration of the protein remaining in the aqueous phase after emulsification (in the serum). The following mass balance relating the adsorption, Γ, with ΔC and the specific surface area of the drops, S (m^2 of oil–water interface per 1 m^3 emulsion), was used to determine the adsorption:

$$\Gamma = \frac{V_C}{S V_{OIL}} \Delta C = \frac{(1-\Phi) d_{32}}{6\Phi} \Delta C \quad (2)$$

where V_C and V_{OIL} are the volumes of the aqueous and oil phases, and Φ is the oil volume fraction. C_{SER} was determined by the method of Bradford [54] or by the BCA-method (for the detailed procedures see Refs. [45,47]).

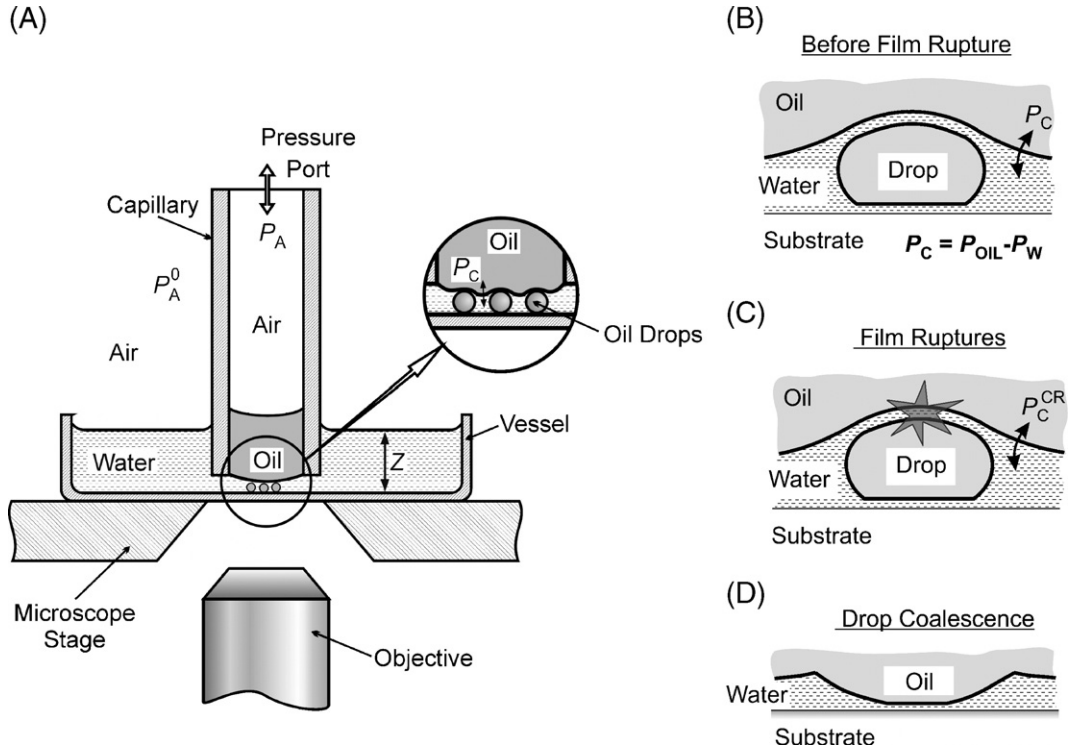

Fig. 3. (A) Basic scheme of the film trapping apparatus and of oil drops trapped between the oil–water interface and the glass substrate (see the magnification lens). (B)–(D) Consecutive stages of the drop-entry process.

2.5. Characterization of drop coalescence

Two techniques were employed for quantitative characterization of emulsion coalescence stability: (1) Film Trapping Technique was used to characterize the coalescence stability of single, micrometer-sized oil drops [44,45,55–57]. This technique was particularly useful for evaluation of the effect of drop size on the coalescence stability. (2) Modification of the classical centrifugation technique [58–62], which allowed us to clarify the effect of various factors on the stability of batch emulsions.

2.5.1. Film trapping technique (FTT)

The operational principle of FTT is illustrated in Fig. 3. A vertical glass capillary, partially filled with oil, was placed just above the bottom of Petri dish. The lower edge of the capillary was immersed in a protein solution, containing dispersed oil drops. The capillary was connected to pressure control system, allowing one to vary and measure precisely the difference, $\Delta P_A = P_A - P_A^0$, between the air pressure in the capillary and the atmospheric pressure. Upon increase of P_A, the oil–water meniscus in the capillary moved towards the glass substrate. When the distance between the oil–water meniscus and the substrate became smaller than the drop diameter, some of the oil drops were trapped in the aqueous film formed between the glass and the upper oil macrophase. By using the pressure control system, P_A was increased until coalescence of the entrapped oil drops with the upper oil phase was observed by an optical microscope. From the measured ΔP_A, one can calculate the capillary pressure of the oil–water interface, which compresses the entrapped drops against the glass substrate, P_C. The capillary pressure at the moment of drop coalescence, P_C^{CR}, is called hereafter "critical capillary pressure for drop coalescence" or, for brevity "barrier to drop coalescence". Higher values of P_C^{CR} correspond to more stable emulsion films and vice versa. Detailed description of the FTT principle and operational procedures is given in Refs. [44,45,55,56].

2.5.2. Centrifugation of batch emulsions

For quantitative characterization of the coalescence stability of batch emulsions, we used centrifugation of 30 vol.% emulsions. The detailed experimental procedure and its verification by various tests are described in Ref. [45]. Briefly, the studied emulsions are tested by centrifugation to determine the acceleration, g_K [m/s^2], at which a thin continuous oil layer is released on top of the emulsion cream as a result of drop coalescence and emulsion decay [44,45]. We use the critical osmotic pressure, P_{OSM}^{CR}, at which this continuous oil layer is released, as a quantitative measure of emulsion coalescence stability. P_{OSM}^{CR} is calculated from the experimental data through the relation [45]:

$$P_{OSM}^{CR} = \Delta\rho g_k \int_0^{H_k} \Phi(z)dz = \Delta\rho g_k (V_{OIL} - V_{REL})/A_{TT} \quad (3)$$

Here $\Delta\rho$ is the difference in the mass densities of the oil and water phases; g_k is the centrifugal acceleration; $\Phi(z)$ is the local volume fraction of oil in the cream (z is the co-ordinate along the centrifugal field, see Fig. 4); V_{OIL} is the total volume of oil in the emulsion; V_{REL} is the volume of released oil on top of the cream; A_{TT} is the cross-sectional area of the test tube.

The theoretical analysis shows [45] that both quantities used to characterize coalescence stability, P_{OSM}^{CR} (measured by centrifugation) and P_C^{CR} (measured by FTT), are equivalent to the pressure jump across the oil–water meniscus compressing the oil drops, $(P_{OIL} - P_W)$, at the moment of drop coalescence with large oil–water interface, cf. Figs. 3B and 4B. In fact, P_{OSM} is exactly equal to the capillary pressure, which squeezes the aqueous film formed between an oil drop, in the uppermost layer of the emulsion cream, and the oil phase released in the course of the centrifugation test. From this viewpoint, P_{OSM}^{CR} and P_C^{CR} characterize one and the same quantity, namely the capillary pressure squeezing the film between a drop and large oil phase, but in different configurations.

2.6. Fourier transform IR-spectroscopy (FTIR)

FTIR spectroscopy was used to detect changes in the secondary structure of the protein molecules upon adsorption, heating, and shelf-storage of solutions and emulsions. For these experiments, soybean oil-in-D_2O emulsions were prepared using a rotor-stator homogenizer, as described in Section 2.2.

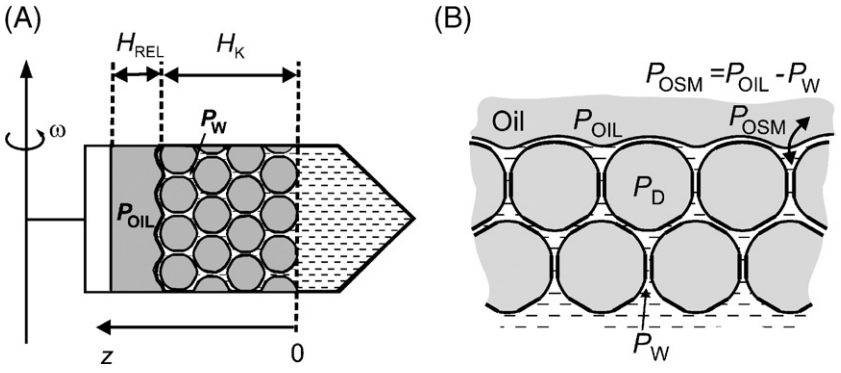

Fig. 4. (A) Equilibrium configuration of an emulsion column in a centrifugal field: H_K is the equilibrium height of the cream, whereas H_{REL} is the height of the layer of released oil, as a result of drop coalescence in the uppermost layer of the cream. (B) Schematic presentation of the boundary layers of emulsion drops in contact with a continuous layer of released oil on top of the emulsion cream. P_D is the pressure inside the drops in the uppermost layer, P_W is the pressure in the neighboring Plateau borders, and P_{OIL} is the pressure in the continuous oil layer.

FTIR spectra were recorded on a Bruker IFS113 FT-IR spectrophotometer, at 20 °C, using 6-reflection ATR cell with TlBr/TlI crystal. Hundred-scan spectra were collected between 4000 and 400 cm^{-1}, in a single-beam mode, with 2 cm^{-1} resolution. The spectra of the aqueous electrolyte solution and of the oil, as well as the bands originating from the water vapors in the 1720–1580 cm^{-1} Amide I region, were subtracted from the spectra of the protein-containing samples to remove all bands unrelated to the protein. The corrected spectra were smoothed using a 13-point Savitsky–Golay method, and the second-derivative spectra were calculated and analyzed.

3. Emulsification in protein solutions — mean drop size and protein adsorption

3.1. Effect of protein concentration

Various experimental studies have shown that at low surfactant concentrations (in the so-called "surfactant-poor" regime [63]), the mean drop size rapidly decreases with the increase of the initial emulsifier concentration [4–8,63,64]. In contrast, at high surfactant concentrations (in the surfactant-rich regime), the mean drop size is independent of surfactant concentration. As illustration of these two regimes, we show in Fig. 5 experimental data for the mean volume-surface diameter, d_{32}, as a function of the initial emulsifier concentration, C_{INI}, for 28 vol.% oil-in-water emulsions, prepared with solutions of whey protein concentrate WPC+150 mM NaCl (Fig. 5A) and SDS (Fig. 5B). Similar dependencies were obtained with the nonionic surfactant Brij 58 [8].

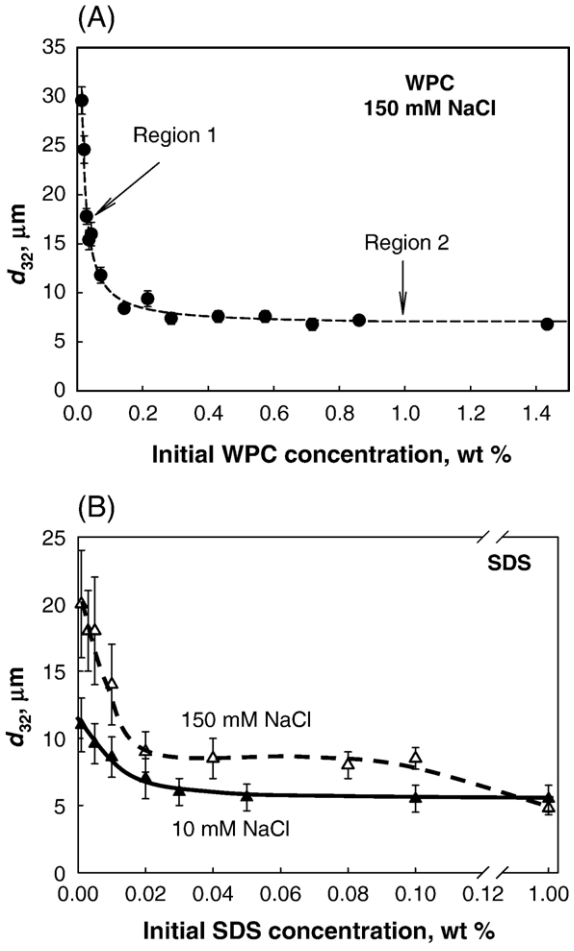

Fig. 5. Mean volume-surface diameter, d_{32}, as a function of the initial emulsifier concentration, C_{INI}, for soybean oil-in-water emulsions stabilized by: (A) WPC and (B) SDS, prepared at $\varepsilon = 2.5 \times 10^5$ J/(kg s) and $\Phi = 0.28$. In Region 1, the mean drop size, d_{32}, is affected strongly by drop coalescence during emulsification, whereas d_{32} in Region 2 is determined by the drop breakup process mainly.

Different factors affect d_{32} in these two regimes of emulsification:

(1) *In the surfactant-rich regime* (denoted as Region 2 in Fig. 5A), the experimental data for d_{32} are described rather well [7,8] by the theory of emulsification in turbulent flow [65,66]. According to this theory, the maximal size, d_K, of the drops formed inside a developed isotropic turbulent flow, can be estimated by comparing the capillary pressure of the drops, P_{CAP}, with the fluctuations of the hydrodynamic pressure, P_T. Most efficient in drop breakup are the turbulent eddies with size comparable to drop diameter. P_T can be expressed through the fluctuations in the fluid velocity, v, and Bernoulli's law [65,66]:

$$P_{CAP} \approx P_T \sim \rho_C \langle v^2(d) \rangle \tag{4}$$

Here ρ_C is the mass density of the continuous phase and $\langle v^2(d) \rangle$ is the mean-square relative velocity between two points, separated by a distance d, in the turbulent flow. For the inertial subrange of sizes of turbulent eddies (in which the inertial forces dominate and the viscous forces acting on the drop surface by the surrounding fluid could be neglected), the mean-square relative velocity could be expressed as [65–67]:

$$\langle v^2(d) \rangle \sim (\varepsilon d)^{2/3} \tag{5}$$

where ε is the rate of energy dissipation per unit mass of the fluid in the emulsification chamber (called also "average power density"). The capillary pressure of drops with diameter d_K can be estimated as:

$$P_{CAP} \sim \sigma_{OW}/d_K \tag{6}$$

where σ_{OW} is the interfacial tension. Combining Eqs. (4)–(6), one obtains the following expression for the maximal drop diameter [65,66]:

$$d_K \sim \varepsilon^{-2/5} \sigma_{OW}^{3/5} \rho_C^{-3/5} \tag{7}$$

Direct comparison of our experimental results for the mean drop size after emulsification, d_{32}, with the predictions of Eq. (7) showed that $d_K \approx d_{32}$, for soybean oil-in-water emulsions, stabilized by WPC, Brij 58, or SDS, in the surfactant-rich regime [8]. As seen from Eq. (7), the main factors affecting the mean drop size in this regime are the interfacial tension, σ_{OW}, and the hydrodynamic conditions during emulsification (expressed through the value of ε). In turn, ε is controlled by the intensity of stirring, viz., by the driving pressure in the valve- and narrow-gap homogenizers or by the rotational speed and size of the impellers in stirred tanks [3–5,8,65–70].

In a recent study [71] we showed that our experimental result $d_K \approx d_{32}$ for soybean oil-in-water emulsions was due to compensation of two opposite effects. First, it was found experimentally and theoretically [66,70,72,73] that for oils with viscosity close to that of water, the mean drop size, d_{32}, should be about half of the Kolmogorov's size, $d_{32} \approx 0.44 d_K$. On the other hand, the viscous dissipation inside viscous oil drops (such as soybean oil) is not entirely negligible in the process of drop breakup, so that the maximal drop size should be larger in comparison with the prediction of Kolmogorov's theory, which neglects the viscous dissipation [73–77]. These two effects compensate each other for oils with viscosity $\eta_O \approx 50$ mPa s, such as the soybean oil and other vegetable triglycerides. For less viscous oils, such as hexadecane with viscosity $\eta_O \approx 3$ mPa s, we obtained experimentally $d_{32} < d_K$, whereas for more viscous silicone oils with $\eta_O > 50$ mPa s we obtained $d_{32} > d_K$, as predicted by the models of Davies [73] and Calabrese [74–76]. For detailed discussion of the effect of oil viscosity on the mean drop size during emulsification, see Refs. [71,73–78].

(2) *In the surfactant-poor regime*, simple phenomenological model was found to describe the experimental data for d_{32} in emulsions, in which no significant electrostatic repulsion between the oil drops was present (prepared with solutions of WPC or Brij 58, and 150 mM NaCl) [7,8].

The main assumption in this model is that the drops coalesce during emulsification, until the emulsifier adsorption on the drop surface reaches a certain threshold value, Γ^*, which is independent of oil volume fraction and intensity of stirring. An additional assumption can be made to simplify the equations, namely, that virtually all emulsifier adsorbs on drop surfaces in the course of emulsification, i.e. $C_{SER} \ll C_{INI}$. These assumptions applied to the mass-balance of the emulsifier used (supposed equal to the adsorbed emulsifier) lead to the following expression for d_{32} [7,8]

$$d_{32} \approx \frac{6\Phi}{(1-\Phi)} \frac{\Gamma^*}{C_{INI}} \tag{8}$$

where C_{INI} is the initial emulsifier concentration in the aqueous phase and Φ is the oil volume fraction. From the slope of the best linear fit of the dependence $d_{32}(1-\Phi)/\Phi$ vs. $1/C_{INI}$ (see Eq. (8) and Fig. 6) we determined $\Gamma^* = 1.9$ mg/m^2 for WPC solutions, which is very close to the protein adsorption in a dense monolayer, $\Gamma_M \approx 2$ mg/m^2, determined from the WPC adsorption isotherm [7]. The application of the same approach to emulsions prepared with Brij 58 + 150 mM NaCl solutions gave $\Gamma^*_{Brij} \approx 1.4$ mg/m^2 [8]. Note that an expression equivalent to Eq. (8) was independently proposed and successfully applied to describe the relation between the mean drop size and the concentration of solid particles in Pickering emulsions, by Arditty and coworkers [79,80].

By combining Eqs. (7) and (8), the following semi-empirical expression was obtained in Ref. [7], which described very well the experimental data for WPC emulsions in the entire range of protein concentrations (in both the surfactant-poor and surfactant-rich regimes):

$$d_{32} \approx d_K + A \frac{\Phi}{(1-\Phi) C_{INI}} \tag{9}$$

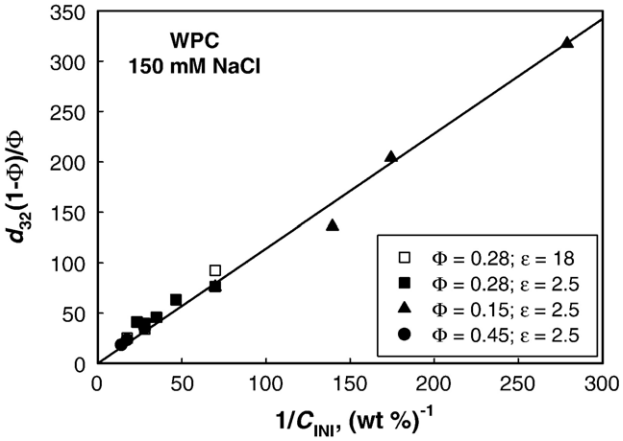

Fig. 6. Normalized volume-surface diameter, $d_{32}(1-\Phi)/\Phi$, as a function of the inverse initial protein concentration, C_{INI}, for emulsions prepared under different emulsification conditions (Φ is the oil volume fraction and ε is given in 10^5 J/kg s). The line is a fit according to Eq. (8).

where d_K is defined by Eq. (7) and $A = 9$ mg/m^2 is a constant, determined from the best fit to the experimental data. The fact that the threshold adsorption Γ^* and the constant A do not depend on Φ, C_{INI}, and ε, shows that Γ^* and A can be considered as characteristics of the emulsifier used [7], and that Eqs. (8) and (9) can be used to predict the mean drop size while varying the oil volume fraction, initial emulsifier concentration and intensity of stirring.

The initial emulsifier concentration, at which a transition between the surfactant-poor and the surfactant-rich regimes occurs, C_{TR}^{INI}, depends on several factors, most important of them being the oil volume fraction and intensity of stirring. C_{TR}^{INI} can be estimated by combining Eqs. (7) and (8):

$$C_{TR}^{INI} \approx \frac{\Gamma^*}{d_K} \frac{6\Phi}{(1-\Phi)} \approx \frac{\Gamma^*}{\varepsilon^{-2/5} \rho_C^{-3/5} \sigma_{OW}^{3/5}} \frac{6\Phi}{(1-\Phi)} \tag{10}$$

In most systems, Γ^* is expected to be between 1.5 and 2.5 mg/m^2. Taking for estimate typical values, $\Gamma^* \approx 2$ mg/m^2, $\rho_C \approx 10^3$ kg/m^3, and $\sigma_{OW} \approx 5$ mN/m, one obtains the following expression for the concentration separating the two regimes of emulsification:

$$C_{TR}^{INI} \approx 1.8 \times 10^{-3} \frac{\Phi}{(1-\Phi)} \varepsilon^{2/5} \tag{11}$$

where C_{TR}^{INI} is expressed in wt.%, and ε is average power density per unit mass. Taking for example $\varepsilon = 2.5 \times 10^5$ J/kg s and $\Phi = 0.3$, which are typical values in our experiments, we obtain $C_{TR}^{INI} \approx 0.11$ wt.%, which agrees very well with the experimental data (see Fig. 5A).

The qualitative difference between the surfactant-poor and surfactant-rich regimes of emulsification can be illustrated by plotting the experimental data for d_{32} vs. protein adsorption Γ, Fig. 7. The two regimes are clearly seen in this plot: In the surfactant-poor regime Γ remains almost constant (≈ 2.0 mg/m^2), whereas d_{32} decreases from 30 down to 10 μm. In the other regime, d_{32} remains constant, whereas Γ increases from 2 up to 7 mg/m^2, indicating the transition from a monolayer to multilayer protein adsorption. In other words, the drop size is governed by

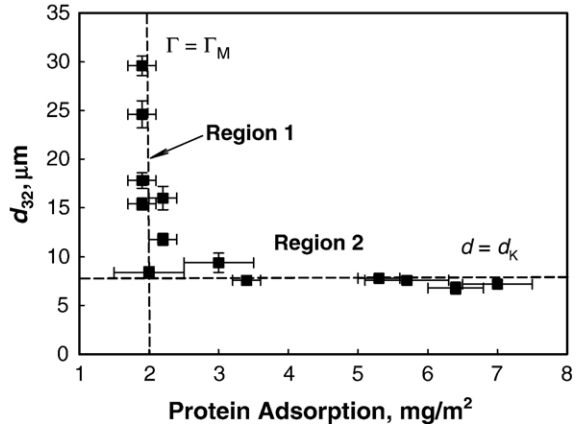

Fig. 7. Mean volume-surface diameter, d_{32}, as a function of protein adsorption, Γ, for WPC-stabilized emulsions prepared at $\varepsilon = 2.5 \times 10^5$ J/(kg s) and $\Phi = 0.28$. Regions 1 and 2 are the same as those shown in Fig. 5 — one sees that in Region 1 the mean drop size varies at fixed protein adsorption, whereas in Region 2 the protein adsorption varies at fixed drop size.

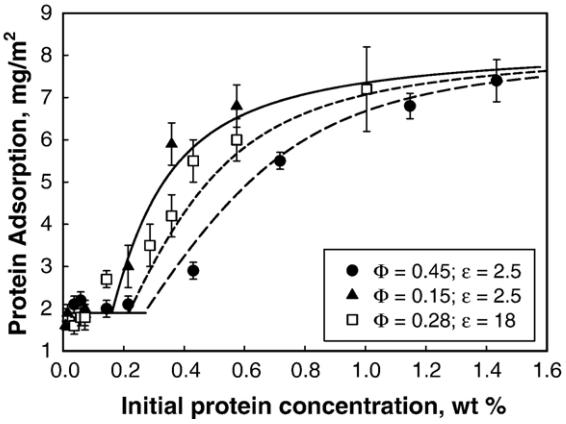

Fig. 8. Protein adsorption as a function of the initial WPC concentration for emulsions prepared under different emulsification conditions (Φ is the oil volume fraction and ε is given in 10^5 J/kg s). The points are experimentally measured data, whereas the curves represent theoretical predictions according to Eqs. (2), (9), and (12).

the protein adsorption at low protein concentrations (Region 1), whereas Γ increases at practically constant drop size at high protein concentrations (Region 2).

The theoretical model outlined above can be further developed by dismissing the assumption that all emulsifier adsorbs on the drop surface during emulsification. In this case, Eq. (2) can be combined with the emulsifier adsorption isotherm, $\Gamma(C_{SER})$, (e.g., the isotherm of Langmuir or Frumkin, presumably known from independent experiments), to obtain a transcendental equation for C_{SER}:

$$\Gamma(C_{SER}) = \frac{(1-\Phi)(C_{INI}-C_{SER})}{6\Phi} d_{32} \tag{12}$$

There are two possible ways to use Eq. (12). In the surfactant-rich regime, the mean drop size can be evaluated from Eq. (7) and introduced into Eq. (12) with some numerical factor relating d_{32} and d_K, if needed (see the discussion after Eq. (7)). After solving Eq. (12) for C_{SER}, one can determine Γ from the adsorption isotherm. Thus one can predict the protein adsorption, Γ, after emulsification under specified conditions, viz. at given C_{INI}, Φ, and ε. The applicability of this approach is illustrated in Fig. 8, where we compare the predicted curves for $\Gamma(C_{INI})$ with experimental data for WPC-stabilized emulsions, obtained at different oil volume fractions and power dissipation rates. An alternative way to use Eq. (12) is to determine experimentally d_{32} (in either of the emulsification regimes) and to introduce the measured value into Eq. (12). This approach was successfully applied in Ref. [8] for SDS-stabilized emulsions to determine Γ at the end of the emulsification procedure.

The theoretical analysis of the emulsification process showed [8] that the relations outlined above are typical for emulsions in which no significant electrostatic repulsion occurs between the dispersed oil drops (i.e. those stabilized by proteins or nonionic surfactants at high electrolyte concentration and/or at the IEP of the protein/surfactant). In such systems, the drops coalesce during emulsification until the emulsifier adsorption becomes equal to Γ^*, so that sufficiently dense adsorption layer is formed, which ensures strong steric repulsion and stabilizes the drops against further coalescence. During subsequent shelf-storage, these emulsions remain stable, which indicates that the adsorption Γ^* is sufficiently high to ensure long-term emulsion stability as well [8]. If a significant electrostatic repulsion exists between the drops during emulsification (e.g., in the presence of ionic surfactants and/or at low electrolyte concentrations), the situation is rather different and this case is considered in the following Section 3.2.

3.2. Effect of electrolyte on the mean drop size during emulsifications

In the *surfactant-rich regime*, the electrolytes affect the mean drop size mainly through the value of σ_{OW}, which enters Kolmogorov's Eq. (7). Thus higher electrolyte concentrations lead to lower values of σ_{OW} (in the case of ionic surfactants), which facilitates the process of drop breakup. As a result, smaller drops are obtained at higher electrolyte concentration in the surfactant-rich regime. Typically, this effect is not very large — see for example the ends of the plateau regions in Fig. 5B (at

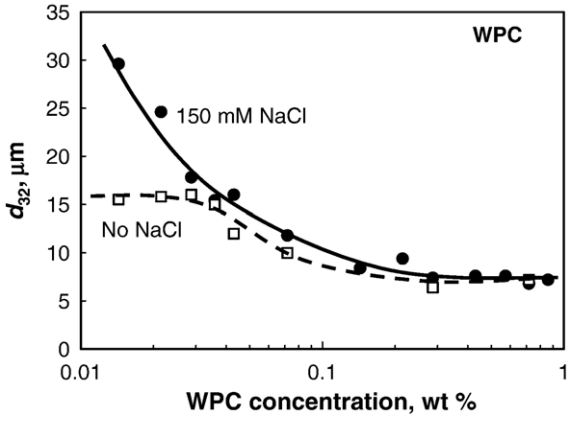

Fig. 9. Mean volume-surface diameter, d_{32}, as a function of the initial WPC concentration, for soybean oil-in-water emulsions prepared at $\Phi = 0.28$ and $\varepsilon = 2.5 \times 10^5$ J/kg s.

1 wt.% SDS), which indicate decrease of d_{32} by about 20% upon addition of 150 mM NaCl to SDS-stabilized emulsion.

In the *surfactant-poor regime*, the effect of electrolyte concentration on the mean drop size can be much stronger. The experimental studies have shown that emulsions containing much smaller drops (in comparison with the prediction of Eq. (8)) are obtained when strong electrostatic repulsion suppresses the drop-drop coalescence during emulsification (see Fig. 9). The experiments show that the drop size in such emulsions falls in the range bounded by the Kolmogorov's Eq. (7) (derived under the assumption of negligible drop-drop coalescence) and Eq. (8), which is derived under the assumption that the drop coalescence has ensured a complete adsorption monolayer on drop surfaces. In other words, in this emulsification regime, the addition of electrolyte in the aqueous phase suppresses the electrostatic repulsion between the drops, thus enhancing their coalescence and shifting the mean drop size from the values predicted by Eq. (7) (negligible coalescence) to the values predicted by Eq. (8) (saturated adsorption layers with $\Gamma=\Gamma^*$).

Interestingly, we found that soybean oil-in-water emulsions containing micrometer-sized drops could be easily obtained with the narrow-gap homogenizer used in the absence of any surfactant, due to strong electrostatic repulsion between the dispersed oil drops, when the aqueous phase contained electrolyte of low concentration ($\leq$10 mM NaCl) (see Fig. 10). However, these emulsions were unstable upon shelf-storage and intense drop coalescence led to complete phase separation within a few minutes after stopping the homogenization procedure.

To describe quantitatively the relation between emulsifier concentration and adsorption on one hand, and the mean drop size, on the other hand, in such electrostatically stabilized emulsions, we estimated the height of the electrostatic barrier preventing drop-drop coalescence during emulsification [8]. For this purpose, Eq. (12) was used to calculate the surfactant (SDS) adsorption at given oil volume fraction, power dissipation rate and emulsifier concentration. Then the surface electric potential of the drops and the resulting electrostatic barrier were estimated using the DLVO theory. Finally, by comparing the theoretically estimated electrostatic barrier and the force pushing the drops against each other upon drop-drop collision in the turbulent flow, we were able to describe the experimental data presented in Fig. 5B — see Ref. [8] for the complete set of experimental data and for the procedure of data interpretation. Both the experimental data and the theoretical model predict that the drop size increases with the increase of the electrolyte concentration in the surfactant-poor regime.

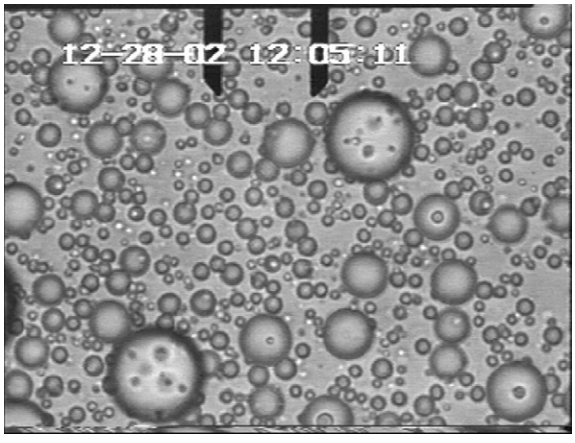

Fig. 10. Photograph of micrometer-sized soybean oil drops, produced by emulsification in turbulent flow in the narrow-gap homogenizer, without using any emulsifier ($\varepsilon=2.5\times10^5$ J/kg s, $\Phi=0.05$, 10 mM NaCl). The oil was pre-purified from surface active contaminants ($\sigma_{OW}=29.5$ mN/m). The obtained emulsion is unstable and the oil phase separates completely within 2–3 min. The distance between the vertical dark bars in the upper part of the photograph is 20 μm.

One particular feature of the electrostatically-stabilized emulsions in the surfactant-poor regime is that the drop coalescence is incomplete during emulsification. The drops formed during emulsification are too small to be covered by a dense protective layer of surfactant/protein molecules. As a result, the drops continue to coalesce after stopping the homogenization, so that bulk oil layer is formed upon shelf-storage on top of the emulsion cream [8].

4. Effect of drop size on coalescence stability and on mode of coalescence

4.1. Effect of drop size on coalescence stability

The effect of drop size on emulsion coalescence stability has been discussed in the literature [1,29,44,45,81–87], but in most studies it interferes with the effect of protein adsorption so that no clear conclusions could be drawn. The reason for the interference of these two effects is that the emulsification procedures usually produce smaller drops at higher emulsifier concentration. At the same time, the adsorption may also increase with the emulsifier concentration [7,8,84–87]. For this reason, the relative contributions of the effects of emulsifier adsorption and drop size on emulsion stability cannot be easily separated [64,83,87].

To clarify the effect of drop size on emulsion coalescence stability we used two techniques. In the Film Trapping Technique (FTT) single, micrometer-sized oil drops are compressed against a large oil phase and the critical capillary pressure leading to drop coalescence is used to characterize the coalescence stability [44,45]. The desired protein adsorption on drop surface is ensured by storing the oil drops in the bulk protein solution for a certain period of time before trapping and compressing them in the wetting film of the FTT equipment [45].

The experimental results obtained for oil drops stabilized by two different protein concentrations (0.005 and 0.01 wt.% BLG), which correspond to different protein adsorptions ($\Gamma=1.35$ and 1.5 mg/m^2, respectively) showed that the larger drops coalesced at lower capillary pressure, P_C^{CR} (i.e. the larger drops are less stable), see Fig. 11A. A simple empirical expression, which implies that $1/P_C^{CR}$ is a linear function of the drop radius, R_0, was found to describe very well the experimental data:

$$1/P_C^{CR} = A + BR_0$$
$$A = 1.13\times10^{-2}Pa^{-1};\ B = 290Pa^{-1}.m^{-1};\ C = 5\times10^{-3}wt\%;\ \Gamma = 1.35mg/m^2$$
$$A = 5.88\times10^{-3}Pa^{-1};\ B = 102Pa^{-1}.m^{-1};\ C = 10^{-2}wt\%;\qquad \Gamma = 1.5mg/m^2 \quad (13)$$

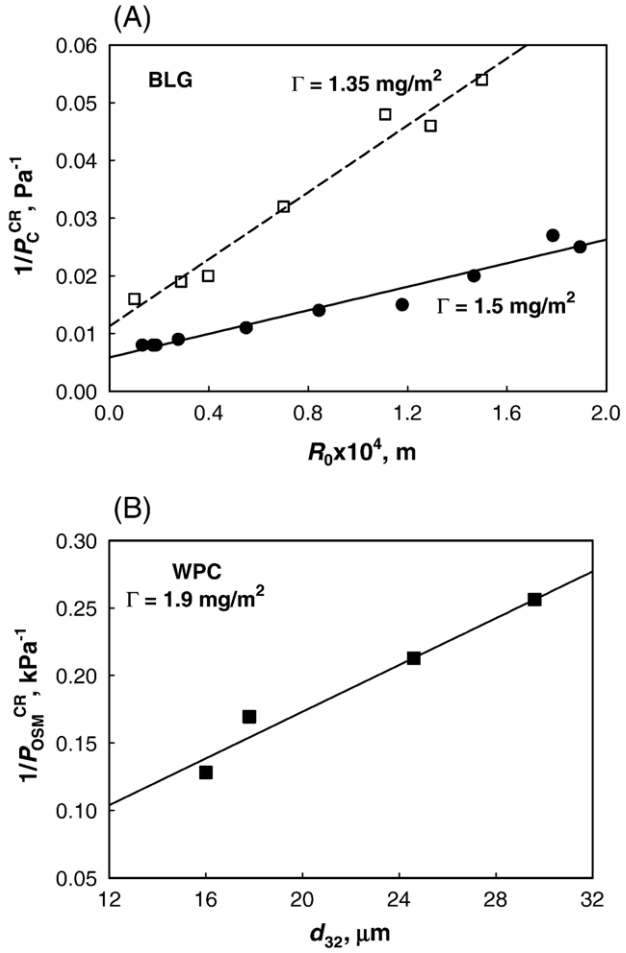

Fig. 11. Dependence of the barrier to drop coalescence on drop size. (A) Measured by FTT with individual drops stabilized by BLG; (B) measured by centrifugation with batch emulsions stabilized by WPC. All solutions are with 150 mM NaCl and natural pH ≈ 6.2.

For large drops ($BR_0 \gg A$), Eq. (13) predicts that P_C^{CR} is a linear function of $1/R_0$:

$$P_C^{CR} \approx 1/(BR_0) \tag{13A}$$

In an independent series of experiments we characterized the coalescence stability of batch emulsions using centrifugation (Section 2.5.2) and found that Eq. (13A) described very well the experimental data for the critical osmotic pressure of WPC-stabilized emulsions at fixed protein adsorption, $\Gamma \approx 1.9$ mg/m^2 (see Fig. 11B) [45]. In these experiments, the constant protein adsorption was ensured by appropriate choice of emulsification conditions [7,45].

A similar linear decrease of the foam stability with the size of the bubbles was reported in Ref. [88]. In separate studies [45,89], Eq. (13A) was found to describe very well the barrier to coalescence of silicone oil drops with air–water interface (studied in relation to the antifoam effect of silicone oils). Therefore, we expect that Eqs. (13) and (13A) are applicable to a wide range of experimental systems.

4.2. Theoretical analysis of the size of liquid films formed at the interface between an emulsion and a solid wall or an oil macrophase

As shown in the previous section, the critical pressure for emulsion film rupture depends on the drop size. In fact, what matters for coalescence stability is the diameter (or the area) of the emulsion film and the capillary pressure driving its thinning, rather than the drop-size itself. A simple phenomenological explanation for the effect of film size is that the larger films are less stable, because the probability for formation of an unstable spot (nucleus of film rupture) increases with the film area. As shown in the current section, the observed drop size dependence of emulsion film stability suggests two possible modes of emulsion destabilization. A theoretical analysis and experimental results illustrating these two modes of emulsion decay are presented below.

In the real batch emulsions, two different in size emulsion films often appear in the upper region of the emulsion column: (1) films formed between two drops of similar size, and (2) films formed between the drops located in the uppermost layer of the emulsion and large oil–water interface (see Fig. 12). A simple force balance shows that the films of type 2 must be larger in area than the films of type 1 for equally sized drops at mechanical equilibrium [44]. To analyze this difference, let us consider theoretically the following two idealized systems: emulsion composed of monodisperse drops, which are arranged in fcc-lattice and are placed in contact with (A) solid wall or (B) bulk oil (Fig. 12).

4.2.1. Emulsion in contact with solid wall

The mechanical equilibrium of a drop situated in the uppermost 1st layer of emulsion drops (Fig. 12A) requires that the repulsive force between the drop and the solid wall, F_W, must be counterbalanced by the vertical projections of the

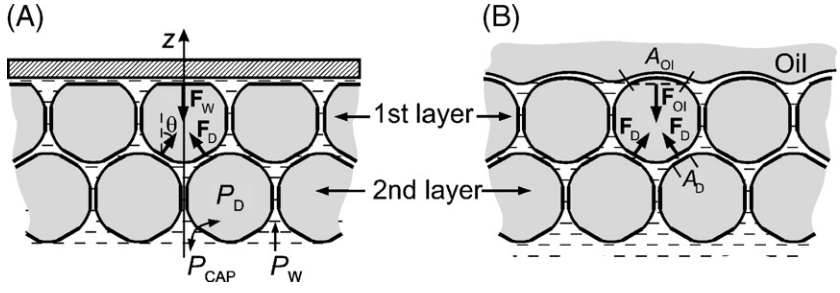

Fig. 12. Schematic presentation of the upper layers of emulsion drops in contact with: (A) solid wall; (B) large oil phase.

forces, F_D, exerted in the contacts of the same drop with its neighbors from the second layer:

$$F_W = mF_D\cos\theta \tag{14}$$

where m is the number of close neighbors located in the second layer of drops, and θ is the angle between the direction of the drop-drop forces and the normal to the solid surface. Both m and θ depend on the particular arrangement of the drops, and in the case of fcc-packing, $m=3$ and $\cos\theta=\cos(\pi/6)\approx 0.816$. On the other hand, the forces F_W and F_D are equal to the product of the respective film area, A_i, and the repulsive disjoining pressure stabilizing the liquid film, Π_i, that is $F_i=\Pi_i A_i$ ($i=W$ or D for the drop-wall or drop-drop film, respectively). In the idealized system of monodisperse drops and a flat solid surface in mechanical equilibrium, all films are planar and the disjoining pressure is exactly equal to the capillary pressure difference between the drops and the surrounding aqueous phase, $\Pi_i=P_{CAP}\equiv P_D-P_W$. Therefore, Eq. (14) can be represented in the form:

$$A_W = A_D m\cos\theta \approx 2.45A_D \qquad \text{3D fcc} - \text{emulsion; solid wall} \tag{15}$$

which shows that the area of the film between the drop and the solid wall is 2.45 times larger than the area of the film between two equally-sized drops. Respectively, the difference in the diameters of these films is $(2.45)^{1/2}\approx 1.57$. This difference is mainly due to the fact that the force, F_W, exerted on a film of type drop-wall must be counterbalanced by the forces, F_D, created by 3 contacts of type drop-drop. Note that Eq. (15) presents only the ratio of the film areas; the actual film size is determined by two other factors as well: drop volume, V_D, and drop volume fraction, Φ [90–93].

4.2.2. Emulsion in contact with large oil phase

The mechanical balance in the case of an emulsion in contact with a large oil phase (e.g., with a continuous layer of oil or with an oil lens of diameter much larger than the size of the individual drops) is more complex, because the films formed between the drops in the uppermost layer and the large phase are curved, Fig. 12B. The disjoining pressure of such a film, Π_{OI}, is given by the expression [55,56]:

$$\Pi_{OI} = P_{OI}\equiv P_F - P_W = P_{OIL} - P_W + \frac{2\sigma_{OW}}{R_F} \tag{16}$$

where P_{OI} by definition is the pressure difference between the water phase inside the film, P_F, and the pressure in the neighboring Plateau border, P_W. The subscript "OI" indicates the contact of the emulsion with a large oil–water interface. R_F is the radius of curvature of this film, and P_{OIL} is the pressure in the oil phase above the drop, see Fig. 12B. As shown by Princen [90], the pressure difference $(P_{OIL}-P_W)$ is exactly equal to the osmotic pressure of the emulsion, P_{OSM}. On the other hand, from the Laplace equation of capillarity one can express the last term in Eq. (16) as [56]:

$$\frac{2\sigma_{OW}}{R_F} = \frac{1}{2}(P_D - P_{OIL}) \tag{17}$$

Combining Eqs. (16)–(17) and taking into account that $P_{CAP}=P_D-P_W$, one obtains:

$$P_{OI} = \frac{1}{2}(P_{OSM}+P_{CAP}) = \frac{P_{OSM}(1+f(\Phi))}{2f(\Phi)} \tag{18}$$

where P_{OSM} is the emulsion osmotic pressure at the top of the cream, P_{CAP} is the capillary pressure of the oil drops in the uppermost layer, and $f(\Phi)$ is the fraction of the interface between the emulsion and the continuous oil phase, which is occupied by films. To derive Eq. (18), we used the relationship between P_{OSM} and P_{CAP}, theoretically established by Princen [91]:

$$P_{CAP} = \frac{P_{OSM}}{f(\Phi)} \tag{19}$$

Making a force balance for a drop in the first layer (see Eq. (18)) and using the relations, $F_i=\Pi_i A_i$, one obtains:

$$A_{OI}/A_D = 2m\cos(\theta)\frac{P_{CAP}}{P_{OSM}+P_{CAP}} = 2m\cos(\theta)\left(\frac{1}{1+f(\Phi)}\right) \tag{20}$$

where A_{OI} is the area of the film formed between the drop and the large oil phase (projected onto the macroscopic interface between the emulsion and the oil phase).

For slightly deformed drops (not very high volume fractions), the numerical value of the function $f(\Phi)\ll 1$, and one obtains $(A_{OI}/A_D)\approx 4.9$, which shows that the films formed with the large oil–water interface are much larger in area than the films between two neighboring drops. For high volume fractions, $\Phi\to 1$, the interfacial fraction occupied by the films $f(\Phi)\to 1$, and Eq. (20) predicts that the ratio of the film areas approaches the value for the contact of an emulsion with a solid wall, $A_{OI}/A_D\approx 2.45$ (cf. Eqs. (15) and (20)).

4.3. Mode of coalescence: drop-drop vs. drop-large oil phase

The emulsion decay in a system, like the one shown in Fig. 12B, could occur in two different modes: (1) as a coalescence of the drops in the uppermost layer of the emulsion cream with an already existing macroscopic oil phase (e.g., macroscopic oil lens or continuous oil layer). This mode of coalescence is termed hereafter "drop-large oil phase coalescence". (2) By a drop-drop coalescence inside the emulsion cream, which leads to formation of larger drops, which further coalesce with each other to eventually release a continuous oil layer on top of the cream [44,45].

With respect to the driving pressure for film thinning, the films formed between two neighboring oil drops inside the cream should be less stable than the films formed between the oil drops and the continuous oil phase. The reason is that the driving pressure for film thinning between two equally-sized drops (which is the capillary pressure of the drops, $P_{CAP}=P_D-P_W$) is higher than the pressure squeezing the emulsion film between an oil drop and a neighboring large oil phase, $P_{OI}=P_F-P_W$ (see Fig. 12B and Eq. (18)). Therefore, with respect to the driving pressure, the coalescence through mode 2 would be favored.

On the other hand, with respect to the film size, the favored mode of emulsion decay should be the coalescence between a drop and the continuous oil phase, i.e. mode 1, because the respective emulsion film has larger area than the film between two equally-sized drops (see Eq. (20)). It is not known in advance which of these two effects would prevail in a specific system and, hence, which is the actual mode of emulsion decay.

An estimate for the relative importance of these two modes of coalescence could be made by employing the experimental observation that the inverse critical pressure for coalescence is a linear function of the drop radius (at equivalent all other conditions) (see Eq. (13) and Fig. 11):

$$\frac{\Pi_{OI}^{CR}}{\Pi_{D}^{CR}} \approx \frac{A + BR_{D}}{A + BR_{OI}} \tag{21}$$

On the other hand, Eqs. (18) and (20) can be expressed in the form

$$\frac{\Pi_{OI}}{\Pi_{D}} = \frac{P_{OSM} + P_{CAP}}{2P_{CAP}} = \frac{1 + f(\Phi)}{2} \tag{18'}$$

$$\frac{R_{D}}{R_{OI}} = \sqrt{\frac{A_{D}}{A_{OI}}} \approx \sqrt{\frac{1 + f(\Phi)}{2m\cos(\theta)}} \tag{20'}$$

Combining Eqs. (18'), (20'), and (21), one derives the following expression for the threshold value, f^{TR}, of the function $f(\Phi)$, which separates the two modes of coalescence:

$$f^{TR} = \frac{A^2 m - B^2 R_{OI}^2 (m - 1/\cos(\theta)) + BR_{OI}\sqrt{[4Am(A + BR_{OI}) + B^2 R_{OI}^2/\cos(\theta)]/\cos(\theta)}}{m(A + BR_{OI})^2} \tag{22}$$

At $f < f^{TR}$, more pronounced will be the coalescence of type drop-drop (the effect of the driving pressure prevails over the effect of drop size), whereas at $f > f^{TR}$ more pronounced will be the coalescence of type drop-large oil phase. Besides, Eq. (22) predicts that if $A \ll BR_{OI}$, the value of $f^{TR} < 0$, which means that the drop-large oil phase coalescence would always be prevailing in such an emulsion. By using the experimentally determined values of A and B (see Eq. (13)), we estimated a threshold value $f^{TR} \approx 0.78$ for the emulsions stabilized by BLG with $\Gamma \approx 1.5$ mg/m^2 and $R_{OI} \approx 20$ μm.

To check whether the two modes of coalescence discussed above occur in real emulsions, we performed centrifugation experiments with emulsions stabilized by 0.01, 0.02, or 0.1 wt.% BLG. In these experiments, the emulsions were centrifuged for 3 h at acceleration, g_K, which was just below the critical acceleration leading to release of bulk oil on top of the emulsion cream. Then, the drop-size distribution in the centrifuged emulsions was compared to that of the original emulsions before centrifugation (see Fig. 13 and Table 1). The results showed that at the lowest BLG concentration, 0.01 wt.%, the mean drop diameter increased very significantly (from 48 to 80 μm) during centrifugation (Fig. 13A). This result suggests that in this system, the leading mode is drop-drop coalescence inside the emulsion cream, which afterwards is followed by release of continuous oil layer. In contrast, the centrifugation did not change significantly the size distribution in the emulsion stabilized by 0.1 wt.% BLG, and the mean drop size remained virtually the same (cf. Fig. 13B and C). Therefore, the prevailing coalescence process in this system was between the drops at the top of the cream and macroscopic oil lenses, which were present in the original emulsion. At the intermediate BLG concentration, 0.02 wt.%, we observed a moderate increase of the mean drop size in the cream (d_{32} increased from 42 to 52 μm), which indicated that both processes, drop-drop and drop-large oil phase, were important.

To compare these experimental results with the theoretical estimate, we calculated the value of $f(\Phi)$ for the studied emulsions, by using the relations between the dimensionless osmotic pressure, $\tilde{P}_{OSM}$, and the function $f(\Phi)$, proposed by Princen [91–93]. The dimensionless osmotic pressure, $\tilde{P}_{OSM}$, is defined as [93]:

$$\tilde{P}_{OSM} = P_{OSM}(R_{32}/\sigma_{OW}) \tag{23}$$

where R_{32} is the mean volume-surface radius ($R_{32} = d_{32}/2$) and σ_{OW} is the oil–water interfacial tension. To evaluate the oil volume fraction, Φ, on top of the emulsion cream in our centrifugation experiments, we used the experimental values of P_{OSM} (see Eq. (3)) and the Princen's dependences of the dimensionless osmotic pressure, $\tilde{P}_{OSM}$, and of the function f on drop volume fraction, Φ [91–93]:

$$\tilde{P}_{OSM} = 0.5842\frac{(1 - 1.892(1 - \Phi)^{1/2})^2}{(1 - \Phi)^{1/2}} \qquad \Phi > 0.99 \tag{24}$$

$$f(\Phi) = (1 - 1.892(1 - \Phi)^{1/2})^2 \qquad \Phi > 0.975 \tag{25}$$

Eqs. (23)–(25) allow us to determine $f(\Phi)$ from the available experimental data. Briefly, the numerical procedure is as follows: P_{OSM}, determined by centrifugation, is introduced into Eq. (23) to calculate the dimensionless pressure, $\tilde{P}_{OSM}$. The latter is used in Eq. (24) to estimate Φ, which, in turn, is introduced into Eq. (25) to determine $f(\Phi)$. The obtained values of $f(\Phi)$ for the studied BLG-emulsions are shown in Table 1.

One can see that the experimental results are in a reasonable agreement with the theoretical prediction. Indeed, for emulsions prepared in 0.01 wt.% BLG solution, where $f(\Phi) \approx 0.29 < f^{TR} = 0.78$, more pronounced is the drop-drop coalescence, as predicted theoretically. For emulsions prepared with 0.1 wt.% BLG solution, the drop-large oil phase coalescence is more pronounced, as predicted ($f(\Phi) = 0.85 > f^{TR}$). The concentration of 0.02 wt.% BLG corresponds to the intermediate regime, in which both modes of coalescence are important.

5. Determination of the dependence $P_{OSM}(\Phi)$ by centrifugation

As shown by Princen [91–93], the emulsion osmotic pressure, P_{OSM}, is a convenient quantity for emulsion characterization,

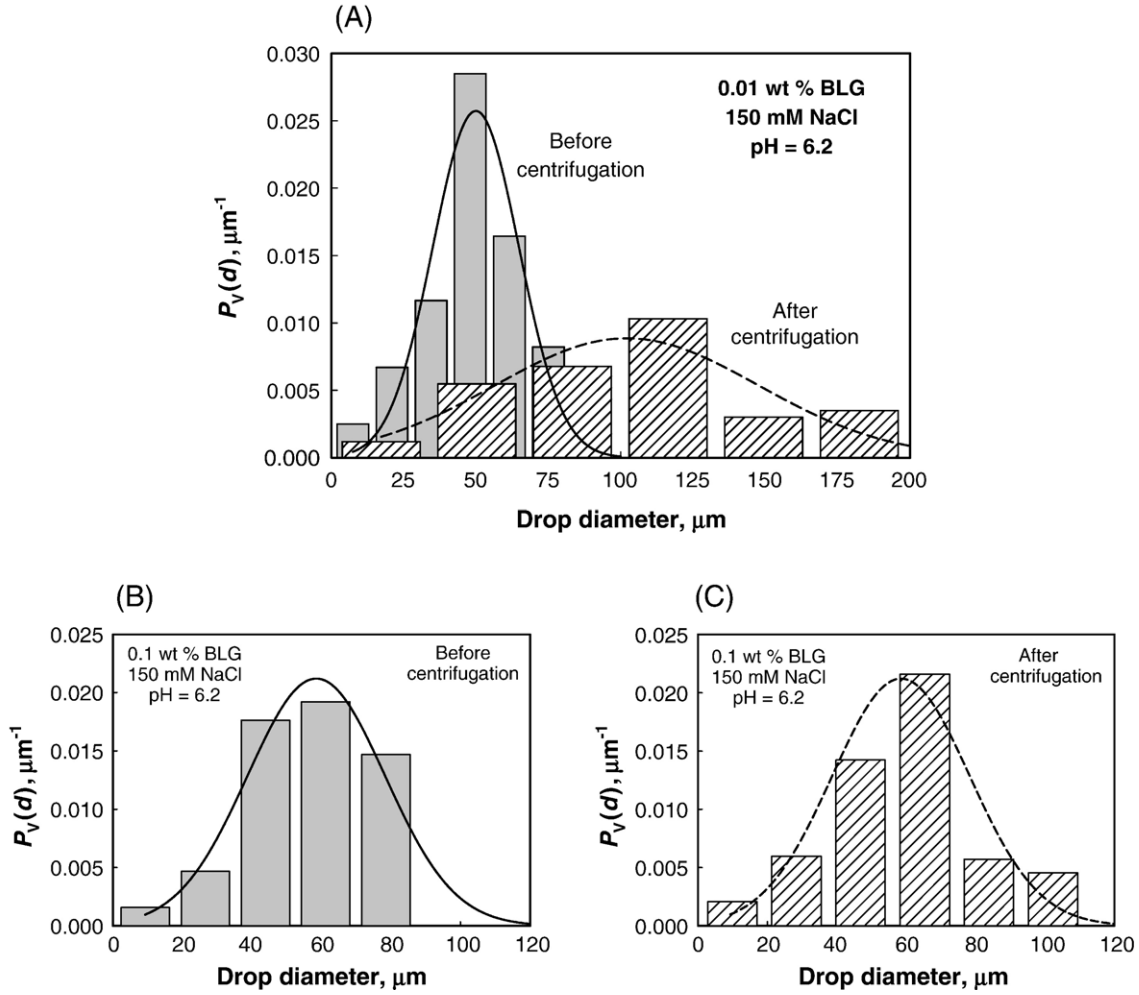

Fig. 13. Drop-size distribution by volume of BLG stabilized emulsions: (A) 0.01 wt.% before and after centrifugation; (B, C) 0.1 wt.% before and after centrifugation, respectively. All solutions are with 150 mM NaCl and pH = 6.2. The centrifugation was made at acceleration, just below the critical one, which would lead to release of continuous oil layer on top of the cream.

because it is amenable to experimental determination and can be rigorously related to various other emulsion properties, such as the equilibrium distribution of emulsion drops in gravitational or centrifugal field, equilibrium vapor pressure of water above a concentrated emulsion, compressibility, etc.

The experimental data about the dependence $\tilde{P}_{OSM}(\Phi)$ are very scarce in the literature, due to serious technical difficulties encountered in the methods used for its determination so far [93,94]. For this reason, we suggest a new, non-destructive procedure for determination of the dependence $\tilde{P}_{OSM}(\Phi)$ by centrifugation, which has several advantages in comparison with the previous procedures. This new procedure and some illustrative results are described in the current section.

5.1. Theoretical basis

The new procedure relies on measuring the equilibrium height of the emulsion cream in the centrifugal test tube, H_k, as a function of the centrifugal acceleration, g_k (the acceleration being below the critical value, which would lead to drop-drop coalescence).

If we assume that the centrifugation field is homogeneous in the emulsion cream, and characterize this field by the average acceleration, g_k [m/s^2], a simple expression can be derived for the equilibrium volume fraction of the oil drops at the top of the cream, $\Phi(H_k)$. To derive this expression we start with the identity

$$H_{OIL} = \int_0^{H_k} \Phi(z)\, dz \tag{26}$$

which expresses the balance of total volume of oil in the cream, V_{OIL}. In Eq. (26), $H_{OIL} = V_{OIL}/A_{TT}$ is the height which the oil would have (placed in a test tube with cross section A_{TT}) if it were completely separated from the aqueous phase. Following

Table 1
Modes of coalescence: dimensionless osmotic pressure, $\tilde{P}_{OSM}$; oil volume fraction on top of the emulsion column, Φ; and fraction of the oil–water interface occupied by films, $f(\Phi)$, for emulsions stabilized by BLG of different concentrations (see Section 4 for explanations)

C_{BLG}, wt.%	Mode of coalescence	$\tilde{P}_{OSM}$	Φ	$f(\Phi)$
0.01	Drop-drop	0.617	0.927	0.29
0.02	Drop-drop and drop-large oil phase	1.38	0.961	0.44
0.1	Drop-large oil phase	12.47	0.998	0.85

Princen [92,93], we assume that Φ is a function only of the dimensionless co-ordinate $\tilde{z}$:

$$\Phi = \Phi(\tilde{z}); \qquad \tilde{z} = \frac{R_{32}}{a_k^2} z = k \frac{R_{32}}{a^2} z \tag{27}$$

where $a_K = (\sigma_{OW}/\Delta\rho g_K)^{1/2}$ is the capillary length in the centrifugal field, $k = g_K/g$ is the relative acceleration (g is the gravity acceleration and a is the respective capillary length), R_{32} is the mean drop radius, and z is the vertical coordinate. The integral in Eq. (26) can be transformed to read

$$H_{OIL} = \frac{a^2}{R_{32}} \frac{1}{k} \int_0^{\tilde{H}_k} \Phi(\tilde{z}) d\tilde{z}; \qquad \tilde{H}_k = k \frac{R_{32}}{a^2} H_k \tag{28}$$

and can be further differentiated with respect to the continuous variable k, which characterizes the centrifugal acceleration

$$\frac{dH_{OIL}}{dk} = \frac{a^2}{R_{32}} \frac{1}{k} \Phi(\tilde{H}_k) \frac{d\tilde{H}_k}{dk} - \frac{a^2}{R_{32}} \frac{1}{k^2} \int_0^{\tilde{H}_k} \Phi(\tilde{z}) d\tilde{z} \tag{29}$$

If the differentiation is made at a fixed total amount of oil, H_{OIL} = const, one derives

$$0 = \frac{a^2}{kR_{32}} \Phi(\tilde{H}_k) \frac{d\tilde{H}_k}{dk} - \frac{1}{k} H_{OIL} \tag{30}$$

which can be rearranged to give the following expression, allowing calculation of the oil volume fraction on top of the cream from the dependence of the cream height on the centrifugal acceleration $H_K(g_K)$

$$\Phi(\tilde{H}_k) = \frac{R_{32}}{a^2} H_{OIL} \left(\frac{d\tilde{H}_k}{dk} \right)^{-1} = \frac{\tilde{H}_{OIL}}{k} \left(\frac{d\tilde{H}_k}{dk} \right)^{-1} \tag{31}$$

The latter expression can be presented in the following equivalent form, which is more convenient for data interpretation:

$$\Phi(H_k) = \frac{H_{OIL}}{H_k \left(1 + \frac{d\ln H_k}{d\ln k} \right)} \tag{32}$$

On the other hand, as shown theoretically by Princen [91–93], the emulsion osmotic pressure at the top of the emulsion column is equal to the buoyancy force (per unit area), which is exerted on the drops by the centrifugal field

$$P_{OSM}(H_k) = \Delta\rho g_k \int_0^{H_k} \Phi(z) dz = \Delta\rho g_k H_{OIL} \tag{33}$$

Finally, eliminating the variable H_k from Eqs. (32) and (33), one can find the sought for relation between P_{OSM} and Φ in parametric form through the variable H_K or k.

Therefore, if a series of experiments are performed at fixed H_{OIL} and variable speed of the rotor (i.e. variable centrifugal acceleration), one can determine experimentally the two functions, $P_{OSM}(\Phi)$ and $\Phi(H_K)$, which are used in the literature [91] to describe the macroscopic equilibrium properties of concentrated emulsions.

5.2. Experimental procedure and data processing

In our experiments, we determined $H(k)$ by optical observation of emulsions during their centrifugation in transparent glass tubes. A binocular lens, stroboscope illumination (Kruss SITE 11), digital CCD camera (Kappa CF 8/1 DX) and video-recorder were used for these observations. The position of the boundary between the emulsion cream and the underlying serum (aqueous phase deprived of oil drops) was precisely determined from the video-records using a capture PC-board and an image analysis software, see Fig. 14. The position of the upper cream–air boundary did not depend on the acceleration, g_k (due to incompressibility of both oil and water), and its position was determined immediately after stopping the centrifuge at the end of the experiment. The distance between the upper and lower boundaries of the cream at a given g_k is equal to H_k.

The procedure for data processing was as follows. (1) Experimentally determined dependence of H on time, t, was extrapolated toward $t \to \infty$ and thus the equilibrium height of the cream, H_k, at a given g_k was obtained. (2) The dependence of H_k on $\ln k$ was constructed. (3) This dependence was interpolated with a continuous empirical function in the entire range of studied accelerations. (4) The interpolation function

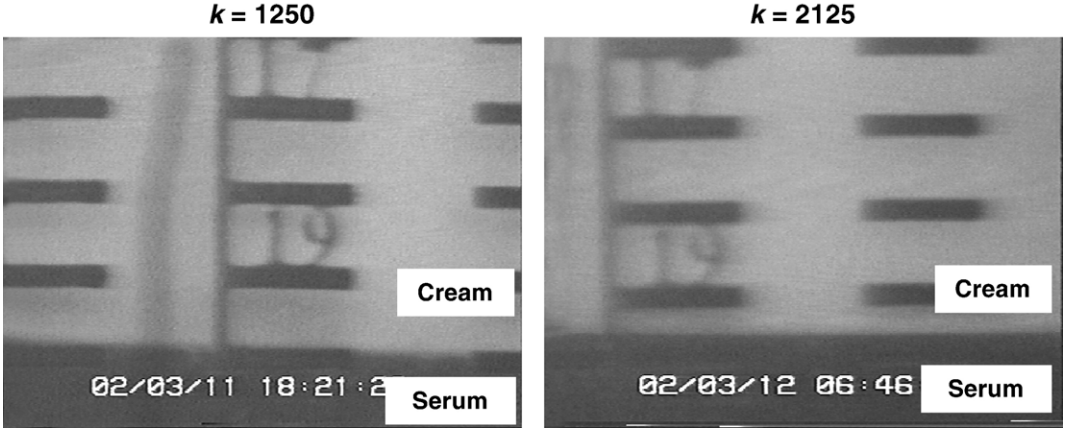

Fig. 14. Photos of the boundary between serum and emulsion cream at two different relative centrifugal accelerations, k.

Table 2
Emulsions studied in Section 5: R_{32} is volume-surface radius, σ is width of drop-size distribution, σ_{OW} is interfacial tension, and $\Delta\rho$ is difference in the mass densities of the oil and water phases

Sample	Emulsifier	Oil phase	R_{32}, μm	σ, μm	σ_{OW}, mN/m	$\Delta\rho\times10^{-3}$, kg/m^3
Emulsion 1	1 wt.% SDS	Hexadecane	6.9	2.9	9.0	0.23
Emulsion 2	2 wt.% SDS	Soybean oil	33	22.5	3.2	0.08

was introduced into Eq. (32) to determine the dependence $\Phi(k)$. (5) From Eqs. (23) and (33) we calculated the dependence $\tilde{P}_{OSM}(k)$. (6) Finally, the dependence $\tilde{P}_{OSM}(\Phi)$ was constructed by eliminating k.

5.3. Experimental results

To illustrate the feasibility of the method, we show the results obtained with two emulsions having different drop-size distributions and compositions — see Table 2 for the emulsion description. Typical dependence of the height of the emulsion cream, $H(t)$, is illustrated in Fig. 15 with the results for emulsion 1, at relative centrifugal acceleration, $k=g_k/g=75$. The experimental curve $H(t)$ consists of two regions — at short times, the height of the cream decreases rapidly and this region is described well by the empirical equation $H(t)=a-bt^{0.5}$, whereas at longer time H decreases exponentially, in agreement with the theoretical predictions of Cox et al. [95]:

$$H(t) = H_k + b_1\exp\left(-\frac{t}{c}\right) \tag{34}$$

The value of the fitting parameter H_K is equal to $H(t\to\infty)$ and is used to construct the dependence $H_k(g_k)$.

In Fig. 16 we plot the experimental data for the dimensionless emulsion height, H_K/H_{OIL}, as a function of ln$k$, for three samples of emulsion 2. The plot shows good reproducibility of the experimental data. By following the procedure described in Section 5.2, we determined the dependence $\tilde{P}_{OSM}(\Phi)$ for the studied emulsions 1 and 2, which is presented in Fig. 17 along

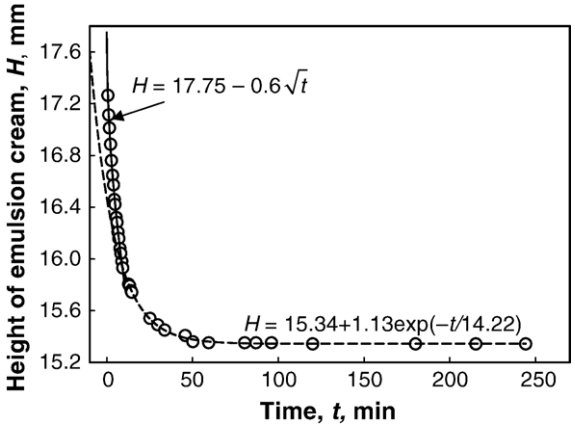

Fig. 15. Height of the emulsion cream as a function of centrifugation time for emulsion 1 (see Table 2 for description) at relative centrifugal acceleration $k=75$. The points are experimental data, whereas the curves are best fits, as explained in Section 5.3.

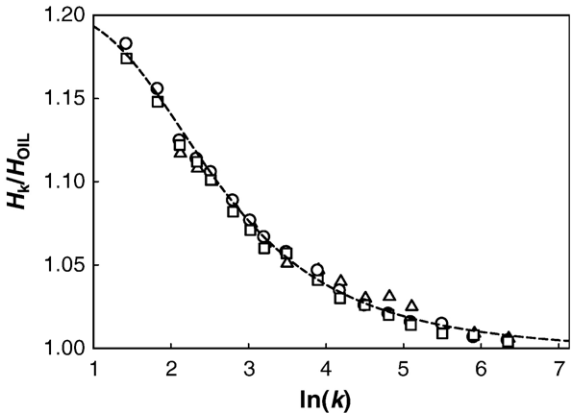

Fig. 16. Dimensionless emulsion height as a function of the dimensionless centrifugal acceleration for emulsion 2 (see Table 2 for its description). The results from three different samples are shown with different symbols to demonstrate the experiment reproducibility.

with the empirical dependence obtained by Princen [93] (the dashed curve) and the theoretical curve for a fcc-packed array of monodisperse emulsion drops [91] (the solid curve). One sees that the experimental points for both emulsions follow relatively well the curves from Refs. [91,93] and that there is some difference between the results for emulsions 1 and 2. This difference is probably related to the fact that emulsion 2 is more polydisperse than emulsion 1 (see Table 2).

In conclusion, the proposed procedure allows one to determine experimentally the functions, $P_{OSM}(\Phi)$ and $\Phi(H)$, which can be used to describe the equilibrium properties of concentrated emulsions [91]. Note that these functions, although determined by this specific method, can be applied generally to emulsions that are not subject to centrifugation, e.g. to homogeneous concentrated emulsions with volume fraction Φ stored in a container, or to emulsions in a gravity field, even if there is no separate bulk aqueous phase below the cream (see e.g., Ref. [93] for the respective explanation).

6. Effects of protein concentration, electrolyte concentration, and pH on β-lactoglobulin adsorption

Protein adsorption on a single air–water interface has been widely studied in the literature by means of different techniques — ellipsometry, neutron reflection, radiolabeling, and others [9–16,96–102]. The effects on protein adsorption of various factors, such as protein concentration, pH, and aging time of the surface were studied. However, the results for a single air–water interface could not be directly applied to the oil–water interface in emulsions. For example, a considerably higher protein adsorption is often reported in experiments with batch emulsions, as compared to the results from ellipsometrical measurements with a single air–water interface, at similar pH and protein concentration [99].

For this reason, we present in this section a summary of our experimental results for the BLG adsorption on the drop surface in the emulsions studied. These results are used in the following sections to interpret the experimental data for emulsion coalescence stability.

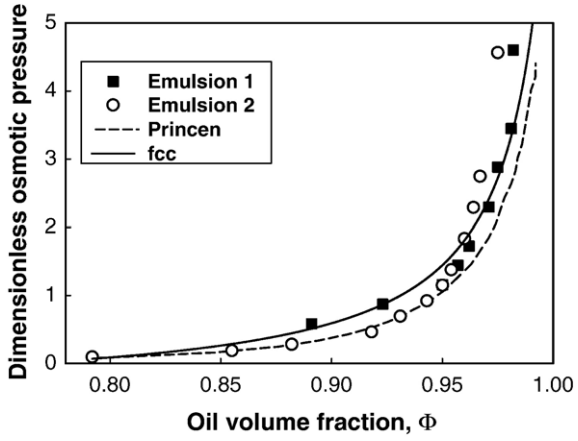

Fig. 17. Dimensionless osmotic pressure, $\tilde{P}_{OSM}$ as a function of the oil volume fraction, determined by the procedure from Section 5. The dashed curve is drawn according to the experimental results by Princen [93], whereas the continuous curve is a theoretical calculation for monodisperse drops ordered in fcc-lattice [91].

6.1. Effect of protein concentration

This series of experiments was performed at $C_{EL}=150$ mM and natural pH=6.2. The BLG adsorption, Γ, is presented in Fig. 18 as a function of protein concentration in the aqueous phase after emulsification (in the serum). In the concentration range between 0.001 and 0.03 wt.%, $\Gamma\approx 1.5\pm 0.1$ mg/m^2, which is close to the values reported in the literature for saturated (dense) adsorption BLG monolayer at an air–water interface ($\Gamma_M\approx 1.65$ mg/m^2 [14,100,102]). A simple geometrical estimate shows that a compact monolayer of intact BLG molecules having approximately spherical shape with diameter 3.58 nm and molecular mass 18,400 g/mol [39,96] would correspond to $\Gamma_{Int}\approx 2.75$ mg/m^2. Therefore, the fact that saturated monolayers are obtained with $\Gamma_M\approx 1.65$ mg/m$^2<\Gamma_{Int}$, indicates that partial unfolding of the BLG molecules occurs upon adsorption at natural pH.

We found that Γ increases at higher protein concentrations and reaches 2.9 mg/m^2 at 0.1 wt.% of BLG [45]. Such high values, $\Gamma>\Gamma_M$, have been already reported in the literature — for instance, one can find the following values for an oil–water or an air–water interface: $\Gamma\approx 2.0$ mg/m^2 [98], 2.4 mg/m^2 [14], and 3.8 mg/m^2 [1,87], at 0.1 wt.% BLG.

To check whether the measured by us value of 2.9 mg/m^2 corresponds to an adsorption multilayer of BLG molecules, we applied the so-called "rinsing procedure" [45]. As shown in the literature [1,29,30,87,103], two types of molecules can be distinguished in the protein adsorption multilayers. The molecules in the first adsorption layer, which is in direct contact with the oil–water interface, are irreversibly adsorbed on the drop surface due to their very high adsorption energy. In contrast, the molecules adsorbed over the first layer are reversibly adsorbed and could be rinsed by replacing the emulsion serum (which is in equilibrium with the adsorption multilayer) with an electrolyte solution deprived of protein [7,45]. By using the rinsing procedure described in Ref. [45], we showed that some fraction of the adsorbed protein is indeed desorbed upon rinsing of the BLG-emulsions with NaCl solution — the initial adsorption of 2.9 mg/m^2 decreased down to 1.6 mg/m^2. Note that the latter value practically coincides with the protein adsorption in a completed monolayer, Γ_M. Thus we can conclude that the emulsion rinse leads to desorption of the excess protein molecules (over Γ_M) and only the first layer remains firmly attached to the drop surface.

In conclusion, protein adsorption monolayer with $\Gamma\approx 1.5$ mg/m$^2\approx 0.9\Gamma_M$ is formed at protein concentration in the serum, C_{SER}, between 0.001 and 0.03 wt.% ($C_{EL}=150$ mM and natural pH=6.2), whereas a multilayer is built up at higher protein concentrations (Fig. 18).

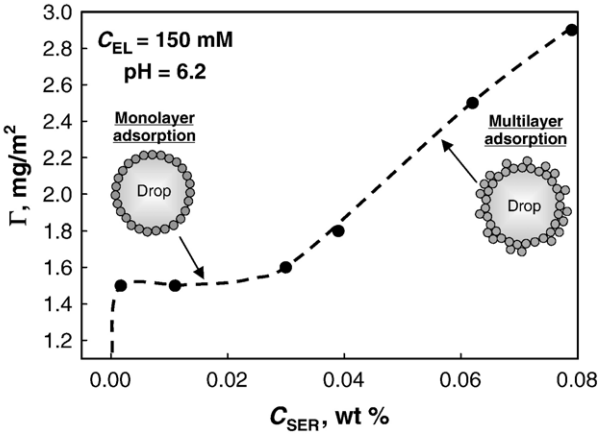

Fig. 18. BLG adsorption on the surface of the emulsion drops, Γ, plotted as a function of the protein concentration in the serum, C_{SER}. The protein solutions contain 150 mM NaCl and 0.01 wt.% NaN_3 (pH=6.2).

6.2. Effect of electrolyte

We studied the effect of C_{EL} on Γ, at natural pH=6.2 and 0.02 or 0.1 wt.% BLG (see Fig. 19). At low electrolyte concentration, $C_{EL}<50$ mM, the protein adsorption $\Gamma\approx 0.9$ mg/m^2 corresponds to a monolayer, with a significant mean distance between the centers of the adsorbed protein molecules at both BLG concentrations (0.02 and 0.1 wt.%), due to electrostatic repulsion between these molecules. At higher electrolyte concentration, $C_{EL}>50$ mM, Γ increases up to 1.65 mg/m^2, due to formation of more compact monolayer, when $C_{BLG}=0.02$ wt.%. A multilayer with $\Gamma>2.5$ mg/m^2 is formed at high

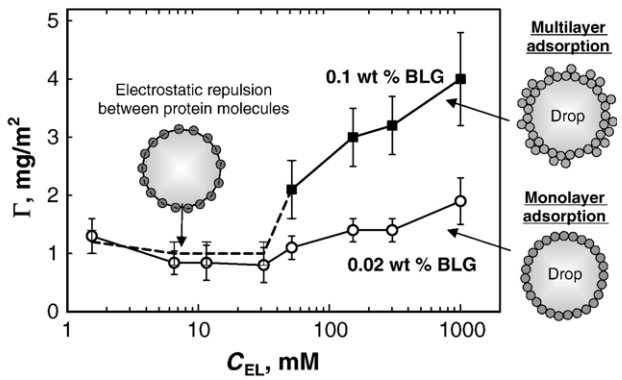

Fig. 19. Protein adsorption, Γ, as a function of electrolyte concentration, C_{EL}, for emulsions stabilized by 0.02 wt % and 0.1 wt % BLG; pH=6.2 (natural).

electrolyte and protein concentrations, $C_{EL}>100$ mM and $C_{BLG}=0.1$ wt.%, as a result of the suppressed electrostatic repulsion between the adsorbed protein molecules (see Fig. 19).

6.3. Effect of pH

The effect of pH on Γ for emulsions stabilized by 0.02 wt.% BLG is shown in Fig. 20. For both electrolyte concentrations studied, $C_{EL}=10$ and 150 mM, the adsorption passes through a maximum, $\Gamma\approx 2.5$ mg/m^2, at pH around the isoelectric point (IEP), due to suppressed electrostatic repulsion between the protein molecules. The rinsing of the emulsion with electrolyte solution showed that this adsorption corresponded to a monolayer — no protein desorption was detected upon rinsing [39]. Therefore, a monolayer with $\Gamma\approx\Gamma_{Int}$ is formed at 0.02 wt. % BLG around the IEP, which is probably composed of intact protein molecules, which do not unfold after adsorption.

The effect of pH on Γ for emulsions stabilized by 0.1 wt.% BLG is also shown in Fig. 20 for $C_{EL}=150$ mM. At this high protein and high electrolyte concentrations, adsorption multilayers were formed in the entire range of pH values studied (between 4 and 6.2). Similar dependencies of Γ on pH were reported in the literature for BLG and other globular proteins adsorbed at oil/water or air/water interface [1,14,87,97].

7. Experimental results about the effects of protein adsorption, electrolyte concentration, and pH on coalescence stability

In this section we present briefly the main experimental results for the short-term emulsion stability (up to 3 h after emulsion preparation), as evaluated by centrifugation [39,44,45]. In the following Section 8 we explain these results by considering the surface forces acting between the emulsion drops.

7.1. Effect of protein adsorption

The stability of oil-in-water emulsions in the protein concentration range from 0.01 to 0.5 wt.% BLG was studied

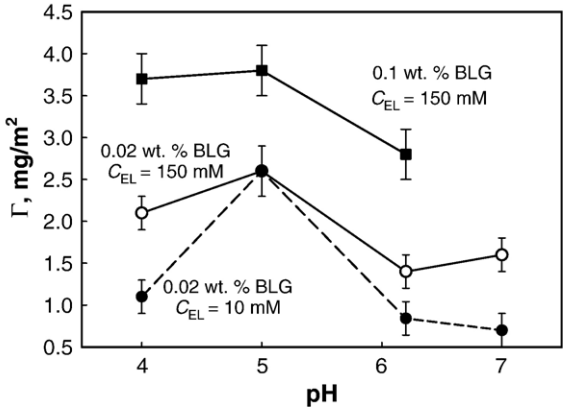

Fig. 20. Protein adsorption, Γ, as a function of pH, for emulsions stabilized by 0.02 wt % BLG at $C_{EL}=10$ mM or 150 mM, and by 0.1 wt % BLG at $C_{EL}=150$ mM.

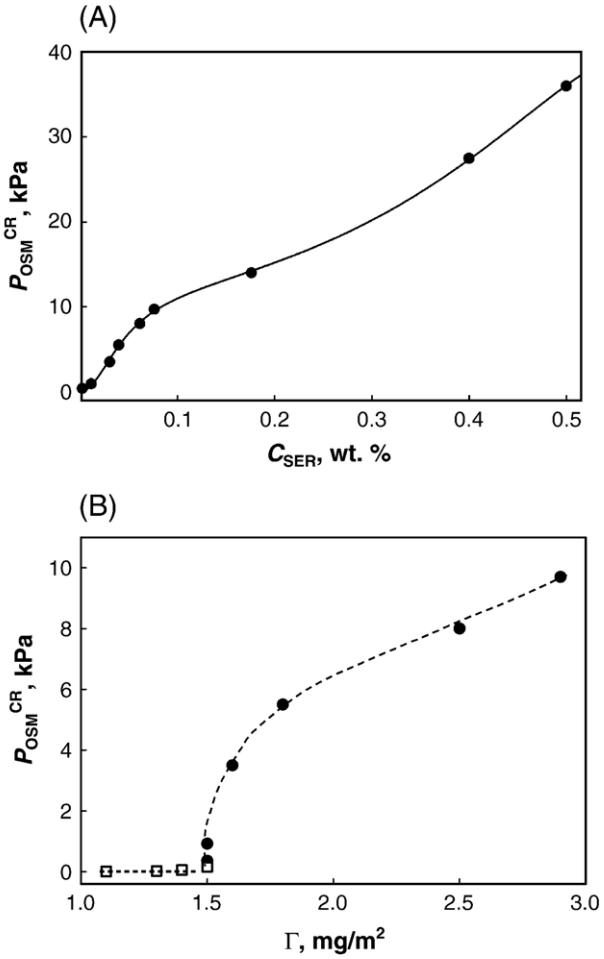

Fig. 21. (A) Critical osmotic pressure as a function of protein concentration in the serum, C_{SER}; (B) critical capillary pressure, P_C^{CR} (measured by FTT, open squares) and critical osmotic pressure, P_{OSM}^{CR}, (measured by centrifugation, solid circles) as functions of BLG adsorption (pH=6.2, 0.15 M NaCl, 0.01 wt.% NaN_3).

at natural pH=6.2 and $C_{EL}=150$ mM [45]. The results for the critical osmotic pressure leading to emulsion decay, P_{OSM}^{CR}, are shown in Fig. 21A, as a function of the protein concentration in the serum, C_{SER}. It is seen that P_{OSM}^{CR} increases significantly (but gradually) with the protein concentration — for an increase of C_{SER} from 0.0017 to 0.5 wt.%, the critical osmotic pressure increases by two orders of magnitude (from 360 to 36,000 Pa).

The same results for P_{OSM}^{CR} are presented in Fig. 21B as a function of the protein adsorption, Γ. As seen from this figure, the emulsions with $\Gamma<1.5$ mg/m^2 are very unstable. There is a very large step-wise increase of emulsions stability at protein adsorption $\Gamma\approx 1.6$ mg/m$^2\approx\Gamma^*$, followed by a more gradual increase of stability at higher adsorptions. Similar experimental results were obtained with WPC-stabilized emulsions as well [36].

The step-wise increase of emulsion stability at $\Gamma^*\approx\Gamma_M$ means that almost a complete protein monolayer should be built on the drop surface to obtain stable emulsions under these conditions (viz. at relatively high electrolyte concentrations). The gradual increase of emulsion stability at higher protein adsorption, $\Gamma>\Gamma_M$, is explained in Section 8.2 by considering the steric repulsion between the protein adsorption multilayers.

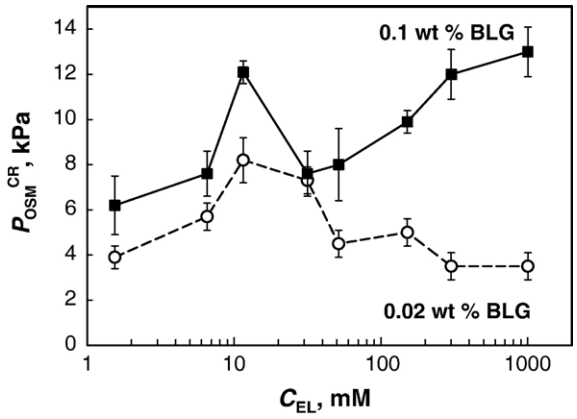

Fig. 22. Critical osmotic pressure for coalescence, P_{OSM}^{CR}, as a function of electrolyte concentration, C_{EL}, in emulsions stabilized by 0.02 wt.% or 0.1 wt.% BLG; pH=6.2.

7.2. Effect of electrolyte

The dependence $P_{OSM}^{CR}(C_{EL})$ is presented in Fig. 22 for the natural pH=6.2 and two BLG concentrations. The stability of emulsions prepared with 0.02 wt.% BLG solutions passes through a maximum around $C_{EL}=10$ mM, followed by a plateau region at high electrolyte concentrations (up to 1 M).

For the emulsions prepared with 0.1 wt.% BLG solutions, the dependence $P_{OSM}^{CR}(C_{EL})$ is somewhat different. At low and moderate electrolyte concentrations, $1.5\ \text{mM} \le C_{EL} \le 50$ mM, the emulsion stability again passes through a maximum, but the stability considerably increases at higher electrolyte concentrations.

The qualitative explanation for the results for $P_{OSM}^{CR}(C_{EL})$ is the following (see Fig. 23). (1) At $C_{EL} \le 50$ mM, emulsion stability is governed by the significant electrostatic repulsion at both BLG concentrations studied. The quantitative comparison of the experimentally obtained and the theoretically calculated electrostatic barriers to drop-drop coalescence, presented in Section 8.1 below, shows that the observed maximum in emulsion stability at $C_{EL} \approx 10$ mM corresponds to a maximum in the interdroplet electrostatic repulsion. (2) For emulsions prepared with 0.1 wt.% BLG solutions, the observed significant increase in emulsion stability at $C_{EL} > 50$ mM is due to formation of protein adsorption multilayer, which leads to efficient steric stabilization of the emulsion films (see Section 8.2). (3) For emulsions prepared with $C_{BLG}=0.02$ wt.%, at $C_{EL} > 50$ mM, emulsion stability is governed by a steric repulsion between adsorption monolayers on the drop surfaces, which ensures $P_{OSM}^{CR} \approx 3.5$ kPa, independently of the electrolyte concentration. Quantitative estimates of the interdroplet surface forces, confirming the occurrence of these three different cases in the studied emulsions, are presented in Section 8.

7.3. Effect of pH

The experiments show that emulsion stability passes through a deep minimum at pH=5.0≈IEP, where the stability is practically the same at both electrolyte concentrations studied, 10 and 150 mM (Fig. 24). The low coalescence stability at pH=5.0, as compared to the natural pH=6.2, cannot be explained by a

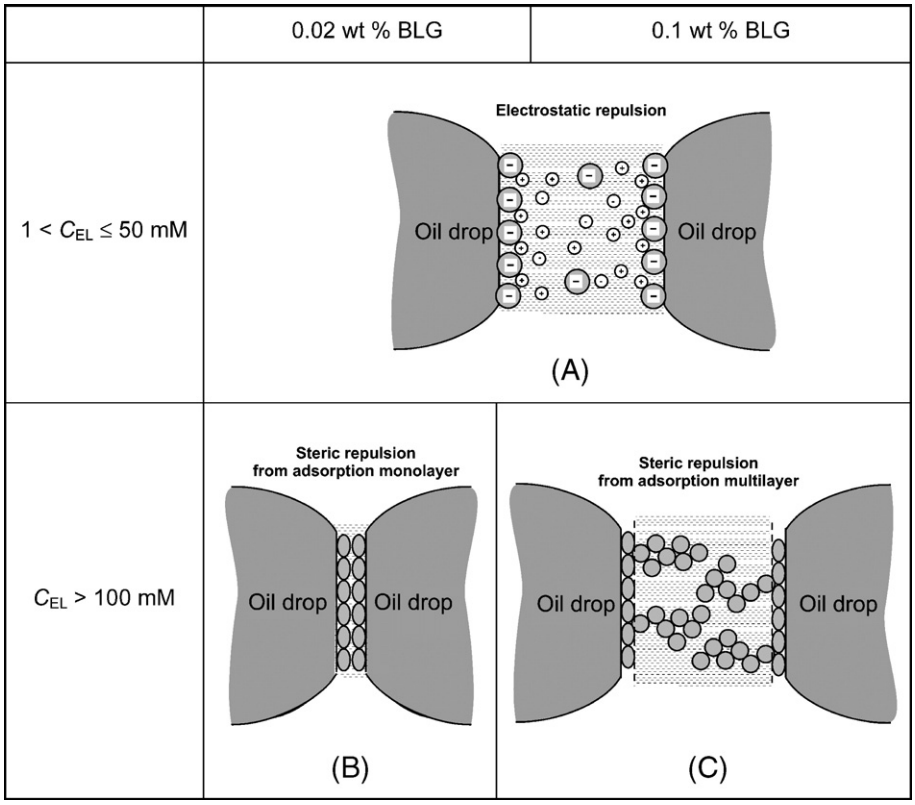

Fig. 23. Schematic presentation of the main types of forces, which govern the coalescence stability of BLG emulsions, at natural pH=6.2.

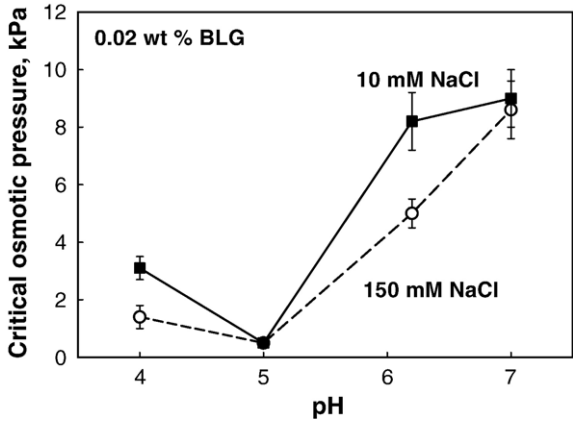

Fig. 24. Critical osmotic pressure for coalescence, P_{OSM}^{CR}, as a function of pH, in emulsions stabilized by 0.02 wt.% BLG, at two different electrolyte concentrations, C_{EL}=10 mM and 150 mM.

reduced protein adsorption, because Γ is maximal at pH=5.0 (cf. Fig. 20). Similar pH dependences were reported in the literature for emulsions stabilized by BLG of higher concentrations (up to 0.4 wt.%) [1,87] and by bovine serum albumin, BSA [30,38].

The most probable explanation for the minimal emulsion stability at pH≈IEP is the formation of an adsorption protein layer of different structure in comparison with the layers formed from charged protein molecules (away from the IEP). One possible explanation is that a relatively rigid adsorption layer is formed at pH≈5.0, which behaves as a fragile/brittle shell that easily ruptures and allows drop-drop coalescence upon small mechanical disturbances of the emulsion. The formation of such brittle protein layers was reported in experiments with emulsion films stabilized by BSA close to its IEP — the films were highly heterogeneous in thickness and easily ruptured (see Fig. 9 in Ref. [104]). Similar explanation for the effect of aging (long-term shelf-storage) on the coalescence stability of emulsions was suggested in Ref. [36] and will be discussed in Section 9 below.

8. Theoretical interpretation of the results for the coalescence stability

8.1. Comparison between the experimental results and theoretical calculations based on the DLVO theory

The van der Waals interaction between two emulsion drops covered with protein adsorption layers was estimated using a three-layer model of the emulsion film, which includes a contribution from the adsorption layer [39,40,105]:

$$\Pi_{VdW} = -\frac{1}{6\pi}\left(\frac{A_{pr-w-pr}}{h^3} - \frac{2A_{o-pr-w}}{(h+\delta)^3} + \frac{A_{o-pr-o}}{(h+2\delta)^3}\right) \quad (35)$$

Here h is the thickness of the aqueous layer inside the emulsion film, δ is the thickness of the adsorbed protein layer ($\delta \approx 3.6$ nm in our case [96]) and A_{ijk} is the Hamaker constant for interaction of phase i with phase k through phase j. The screening of the zero-frequency component of the Hamaker constant by the electrolyte was taken into account [39].

To calculate the electrostatic component of the disjoining pressure, $\Pi_{EL}(h)$, the following expression [106] was used:

$$\Pi_{EL} = 4n_0 k_B T \cot^2\theta, \;\; \kappa h = 2F(\varphi,\theta)\sin\theta \quad (36)$$

where n_0 is electrolyte number concentration, k_BT is thermal energy, κ is inverse Debye screening length, and $F(\varphi, \theta)$ is elliptic integral of first kind. Calculations were made under the assumption of fixed electrical surface potential of the drops, Ψ_S, or fixed surface charge [39]. It was shown in Ref. [39] that Ψ_S could be taken approximately equal to the experimentally determined ζ-potential of the emulsion drops. Following the DLVO model, the disjoining pressure in the emulsion films was considered as a superposition of the van der Waals and electrostatic contributions [105–107]:

$$\Pi = \Pi_{VdW} + \Pi_{EL} \quad (37)$$

From the $\Pi(h)$ isotherms we calculated the height of the electrostatic barrier, Π_{MAX}, which is compared in Fig. 25 with the experimental values of P_{OI}^{CR}, determined by centrifugation.

The points in Fig. 25 show the experimental values of P_{OI}^{CR} vs. C_{EL}, at pH=6.2 and C_{BLG}=0.02 wt.%, whereas the dashed curve shows the theoretically calculated dependence of Π_{MAX} on C_{EL}. As seen from Fig. 25, the DLVO theory adequately describes, at least qualitatively (the theoretical estimated values are around 2.5 higher than the experimentally determined ones), the experimental dependence of emulsion stability on electrolyte concentration at C_{EL}<100 mM. Thus we can conclude that the stability of BLG emulsions at low and moderate electrolyte concentrations is mainly governed by electrostatic repulsion between the drop surfaces. On the other hand, the electrostatic repulsion could not explain the emulsion stability at C_{EL}>100 mM, because the electrostatic barrier disappears (due to lower surface potential and shorter Debye screening length, κ^{-1}).

At the present moment we have no quantitative way to describe emulsion stability in emulsions with monolayer protein adsorption and suppressed electrostatic repulsion (C_{BLG}=0.02 wt.% and C_{EL}>100 mM). The experimental

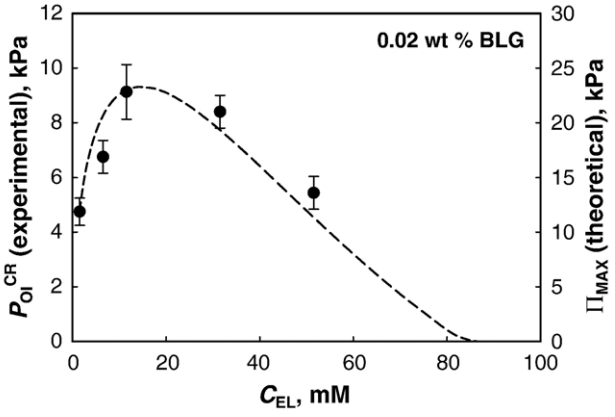

Fig. 25. Experimentally determined dependence of the critical capillary pressure, P_{OI}^{CR}, on C_{EL}, for emulsions stabilized by 0.02 wt.% BLG, along with the theoretical dependence of Π_{MAX} vs. C_{EL} from the DLVO theory (dashed curve). The experimental points are associated with the left-hand-side ordinate, whereas the theoretical curve is associated with the right-hand-side ordinate.

data in Fig. 22 show that the coalescence stability does not depend on electrolyte concentration in these emulsions, $P_{OSM}^{CR}=3.5\pm1$ kPa. We assume that under these conditions there is a direct contact between the protein monolayers adsorbed on the two opposite surfaces of the emulsion films (Fig. 23B). For the factors affecting the stability of these emulsions and the possible mechanisms of drop coalescence, see Section 11.

The experimental results in Fig. 22 show that, at $C_{EL}>100$ mM, the stability of emulsions containing 0.1 wt.% BLG (multilayer protein adsorption) is much higher than the stability of emulsions containing 0.02 wt.% protein (monolayer adsorption). As shown in the following Section 8.2, the coalescence stability at 0.1 wt.% BLG can be explained by considering the steric repulsion between the protein adsorption multilayers.

8.2. Comparison of P_{OI}^{CR} with Π_{MAX}, calculated by including steric repulsion

One can find in the literature a large number of theoretical models for the steric repulsion between polymer layers [105,107–110]. These models differ mainly in the assumed type of solvent–polymer interaction and in the complexity of calculations involved. It was shown in Ref. [111] that an expression, derived originally by Dolan and Edwards [108] for theta-solvents, could be used to describe reasonably well the data obtained with thin emulsion films stabilized by BLG:

$$\Pi_{ST}=\frac{36\Gamma_T k_B T}{L}\exp(-h/L) \tag{38}$$

Here L is the characteristic distance of steric repulsion (for polymer chains it is equal to their radius of gyration, R_g) and Γ_T is the number density of chains per unit area of the adsorption layer.

To adapt this model to our system, we suppose that only protein aggregates adsorbed in the second adsorption layer (which is not in direct contact with the oil–water interface) contribute to the long-ranged steric repulsion. In other words, we consider the first adsorption layer of protein molecules as a substrate over which chains of protein aggregates are attached (see Fig. 23C). To avoid the necessity of using any unknown adjustable parameter, we made the simplifying assumption that the protein aggregates could be modeled as chains, formed by reversible aggregation of BLG molecules. Then we estimated the number concentration of protein aggregates, Γ_T, from the experimental data for protein adsorption, Γ. The fact that the mean number of molecules assembled in one protein aggregate could vary with the protein concentration was accounted for by using the thermodynamic theory of self-assembly [105] — see Ref. [39] for detailed explanations.

The total disjoining pressure was presented as a superposition of the surface forces:

$$\Pi=\Pi_{VdW}+\Pi_{EL}+\Pi_{ST} \tag{39}$$

In Table 3 we present the calculated parameters characterizing the steric interaction, the barriers in the disjoining pressure isotherm, Π_{MAX}, and the experimentally determined values of P_{OI}^{CR} for the systems with multilayer BLG adsorption (high electrolyte and protein concentrations). As seen from the last two columns in Table 3, the values of Π_{MAX} and P_{OI}^{CR} agree very well (difference $\leq15\%$) for all BLG concentrations studied, without using any adjustable parameters in the calculations. This comparison shows that the observed significant increase in emulsion stability at high electrolyte and protein concentrations (see Fig. 22), could be explained with a steric repulsion between adsorbed protein aggregates (Fig. 23C).

In conclusion, the comparison of the experimental results with the theoretical estimates allowed us to distinguish the following qualitatively different cases in the short-term stability of BLG-containing emulsions (see Fig. 23): (1) electrostatically stabilized emulsions with monolayer adsorption; (2) emulsions stabilized by a steric repulsion created by protein adsorption multilayers; and (3) emulsions stabilized by a steric repulsion created by adsorption monolayers. The coalescence stability of emulsions type 1 can be reasonably well described by the DLVO theory. The stability of emulsions type 2 is described by a simple model which accounts for the steric+DLVO interactions. Further experimental and theoretical efforts are needed to reveal the main factors which determine the stability of emulsions of type 3.

9. Effect of storage time and thermal treatment on emulsion coalescence stability

As known from literature, the protein molecules usually change their conformation after adsorption and/or thermal treatment, and this leads to modifications in the properties of the adsorption layers [34,35,112–118]. In the current section, we present experimental results for the effects of storage time and heating on emulsion coalescence stability. To characterize the conformational changes of the protein molecules, and their relation to emulsion stability, we recorded and analyzed FTIR spectra from fresh, aged and heated emulsions and BLG solutions.

9.1. Effect of storage time

The coalescence stability of emulsions prepared at $C_{EL}=150$ mM and pH=6.2 was studied as a function of the shelf-storage period. Fig. 26A presents the results for 0.02 wt.% BLG. Three different stages in the emulsion evolution are distinguished: (1) fast increase of emulsion stability for storage times between 1

Table 3
Comparison of theoretically calculated values of the barrier, Π_{MAX}, with experimentally determined values of P_{OI}^{CR}, at different protein and electrolyte concentrations and natural pH=6.2

C_{EL}, mM	C_{BLG}, wt.%	Γ, mg/m^2	$\Gamma_T\times10^3$, nm^{-2}	Π_{MAX}, kPa	P_{OI}^{CR}, kPa
150	0.08	2.5±0.3	1.14	6.8	8.0±1.0
	0.1	3.0±0.5	1.55	10.5	10.7±0.5
300	0.1	3.2±0.8	1.8	12.3	12.7±1.0
1000	0.1	4.0±0.8	2.2	15.3	13.8±1.0

Γ is experimentally determined protein adsorption; Γ_T is estimated number concentration of protein aggregates on drop surface.

and 5 min; (2) plateau of almost constant stability between ca. 5 and 180 min; (3) significant decrease of emulsion stability, by about 30%, at longer times of storage [36].

Significant changes in the stability with storage time were observed also for 0.1 wt.% BLG emulsions, but several important differences (in comparison with 0.02 wt.% BLG) were noticed (see Fig. 26B). The first stage of rapid stability increase is almost missing, whereas during the third stage the stability decreases by more than 4 times (cf. Fig. 26A and B). In other words, the initial increase of emulsion stability is more pronounced at the lower protein concentration, while the subsequent loss of stability is much more pronounced at the higher protein concentration. As shown in Fig. 18, an adsorption monolayer is formed at 0.02 wt.%, whereas a multilayer is formed at 0.1 wt.% BLG. Therefore, the aging effect (loss of emulsion stability upon shelf-storage) is more pronounced for emulsion drops covered by BLG adsorption multilayers. In Ref. [46], the aging effect was detected also by controlled shearing of fresh and aged emulsions — a significant increase of the mean drop size as a result of drop-drop coalescence during shear was found in aged samples only.

Let us explain briefly the observed stages in the evolution of emulsion stability with time. The initial stage of rapid increase

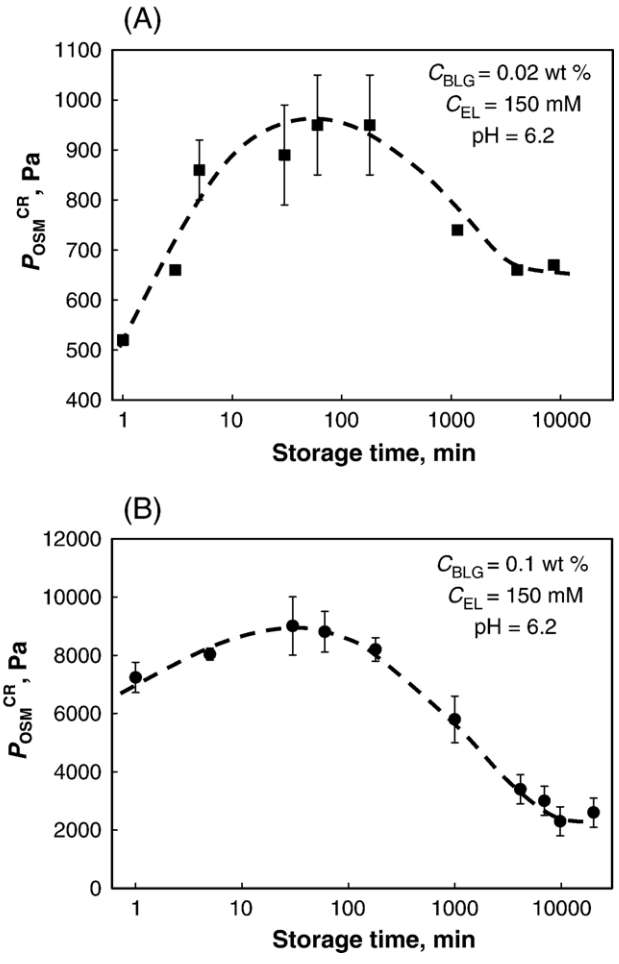

Fig. 26. Critical osmotic pressure, P_{OSM}^{CR}, as a function of storage time for emulsions stabilized by BLG with concentration: (A) 0.02 wt.%, (B) 0.1 wt.%.

of P_{OSM}^{CR} is probably due to a continuing building of the adsorption layers on drop surface during the first several minutes after emulsification. Indeed, we measured a detectable increase of protein adsorption, from 1.25±0.1 to 1.55±0.1 mg/m^2, during the first 30 min after emulsion preparation at 0.02 wt.% BLG. No such change was detected for emulsions prepared with 0.1 wt.% BLG, which explains why the initial increase of stability is less pronounced in this system.

Remarkably, at storage times longer than 30 min, we did not detect any tendency for increase or decrease of Γ for both 0.02 and 0.1 wt.% BLG systems. The measured drop size distributions were virtually the same for fresh and aged emulsions. Therefore, the decrease in emulsion stability at long storage times (during the third stage) could not be explained by changes in the amount of adsorbed protein or in the drop size. These results mean that the aging effect is due to changes in the structure of the protein adsorption layer, which make it less efficient in emulsion stabilization.

The most probable explanation for the aging effect is the formation of intermolecular bonds between the adsorbed protein molecules (see Fig. 27), which transform the adsorption layer into a fragile/brittle shell, which ruptures upon surface expansion and deformation. As illustrated in Fig. 1 and explained in Ref. [45], the formation and expansion of an emulsion film at the point of contact between two drops is accompanied by expansion of the drop surface as well. If the adsorption layer is brittle, then bare (deprived of protein) oil–water spots could appear on the film surfaces, leading to film destabilization and drop-drop coalescence.

The above explanation is in agreement with the experimental results by Murray et al. [34], who studied the rheological properties of BLG adsorption layers, by the Langmuir trough, as a function of aging time [34]. It was shown that the elasticity of the BLG adsorption layers increased with time, and the consequent expansion of the interface led to slower relaxation of the surface tension. These results were explained in Ref. [34] with the formation of robust surface aggregates, which prevented further adsorption of protein molecules on the interface [34].

To check the effect of the formation of intermolecular bonds in the adsorption layer on emulsion aging, we performed emulsion stability tests in the presence of additives. First, we checked what was the role of covalent intermolecular disulfide bonds (S–S bonds) on the aging effect. For this purpose, we performed centrifugation experiments to evaluate emulsion stability (immediately after emulsification and after shelf-storage) in the presence of 10 mM dithiothreitol (DTT) — a reducing reagent known to block the formation of S–S bonds between protein molecules [119]. We found that DTT had no any significant effect on emulsion stability, which means that the aging effect is not related to formation of S–S bonds in the adsorption layer.

The role of non-covalent interactions was tested by addition to the aqueous phase of 4 M urea, which is a reagent known to break the hydrogen bonds (H-bonds) and to suppress the formation of hydrophobic bonds between the protein molecules. The results for emulsion stability at three different concentrations of urea are presented in Table 4. As one can see, the short-term

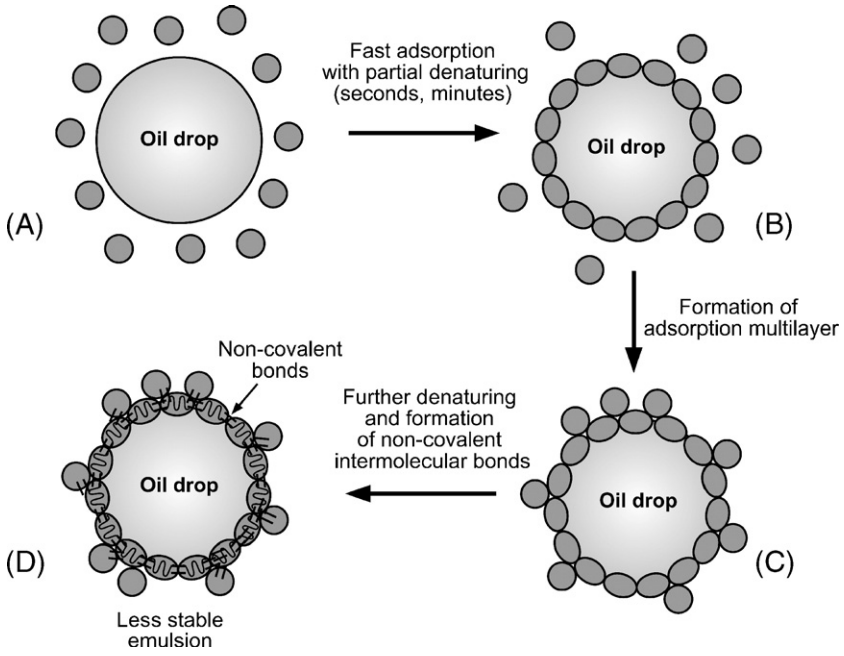

Fig. 27. Schematic presentation of the processes which occur in the adsorption layer during: (A–C) emulsification, (C–D) shelf-storage.

emulsion stability increases with the increase of the urea concentration. Furthermore, the addition of 4 M urea prevents completely the aging effect. As shown by Pace and Tanford [120], the addition of 4.4 M urea in aqueous solutions of BLG has only a little effect on the dissolved molecules at 22 °C — no significant denaturing is induced by urea at this concentration. This means that in our experiments, in which 4 or even 3 M urea affect significantly the emulsion stability, the urea acts exclusively on the unfolded protein molecules in the adsorption layer.

Thus we can conclude that the aging effect is related to formation of non-covalent hydrogen and hydrophobic bonds between the adsorbed protein molecules. This hypothesis is supported by the FTIR spectra discussed in Section 9.3 below (see also Ref. [113]).

9.2. Effect of thermal treatment

The thermal treatment is another procedure known to cause conformational changes and formation of intermolecular bonds in the protein adsorption layers [113,117,119,121].

To check how the heating affected the short-term and long-term stability of BLG-containing emulsions, several series of experiments with heated emulsions were performed. These emulsions were prepared by the following protocol: (1) the temperature of freshly prepared emulsions was raised up to the desired temperature for about 15 min using a thermostat; (2) the emulsions were stored at the desired temperature for 10 min; (3) the emulsions were removed from the thermostat and stored at room temperature for up to 6 days; (4) during the storage period, emulsion samples were centrifuged to characterize their coalescence stability. In parallel, the protein adsorption was determined in separate emulsion samples, prepared under equivalent conditions.

9.2.1. Effect of heating temperature on the coalescence stability of BLG-emulsions

In these experiments P_{OSM}^{CR} and Γ were measured as functions of heating temperature (0.1 wt.% BLG, $C_{EL}=150$ mM, pH=6.2). As seen from Fig. 28, the emulsion heating at $T\leq 78$ °C leads to only slight increase of P_{OSM}^{CR} (less than 30%), whereas heating at $T=85$ and 90 °C increases emulsion stability by more than 4 times, $P_{OSM}^{CR}=40\pm4$ kPa. These results show that the main protein transformation in the adsorption layers occurred between 78 and 85 °C (for the selected heating period of 10 min). The protein adsorption also increases in a step-wise manner with the heating temperature: in emulsions heated at $T=78$ °C, Γ is practically the same as in the non-heated emulsions (2.8 mg/m^2), whereas it increases up to 3.8 mg/m^2 after heating at $T=85$ and 90 °C (similar increase in Γ after heating was reported in Refs. [114,121]). Thus, the increased emulsion stability after heating at $T=85$ °C is at least partially due to increased steric repulsion between the protein adsorption layers. Note that similar adsorption, $\Gamma\approx4.0$ mg/m^2, is measured in non-heated emulsions prepared at $C_{EL}=1$ M (see Table 3), while their coalescence stability, $P_{OSM}^{CR}\approx14$ kPa, is much lower than the stability of the heated emulsions, $P_{OSM}^{CR}\approx40$ kPa. Therefore, the emulsion stability after heating is further enhanced by changes in the structure of the protein adsorption layer.

Table 4
Critical osmotic pressure, P_{OSM}^{CR}, of emulsions stabilized by 0.01 wt.% BLG in the presence of urea ($C_{EL}=150$ mM, pH=6.2)

Storage time	P_{OSM}^{CR}, kPa			
	No urea	3 M urea	4 M urea	6 M urea
30 min	9.7±1.3	20±1.5	26.7±1.5	25±1.5
24 h	2.5±0.5	16±1.5	25.7±1.5	25±1.5
6 days	2.0±0.3	Not measured	25.7±1.5	25±1.5

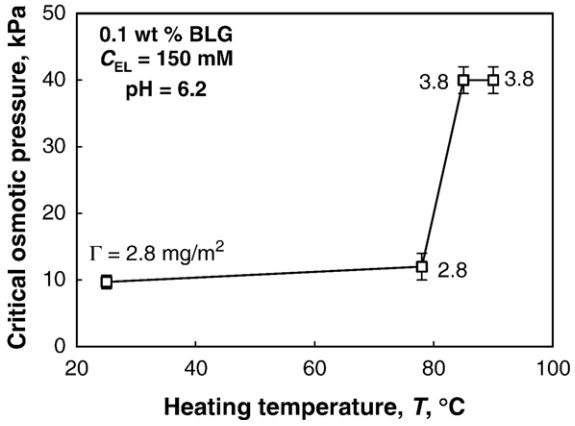

Fig. 28. Effect of heating temperature on the critical osmotic pressure for emulsions stabilized by 0.1 wt.% BLG, at C_{EL}=150 mM and pH=6.2. The numbers associated with the points show protein adsorption in mg/m^2.

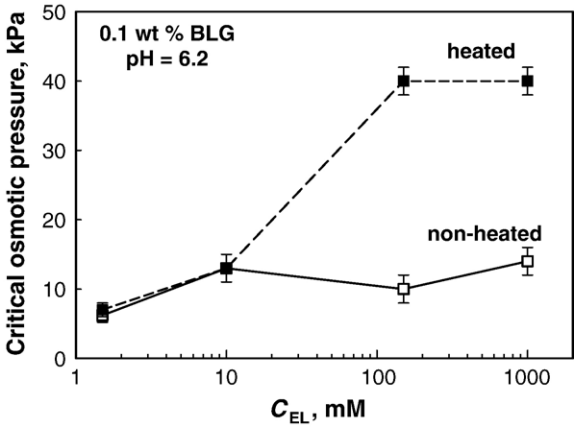

Fig. 29. Critical osmotic pressure as a function of electrolyte concentration, C_{EL}, for non-heated and heated at 85 °C emulsions, stabilized by 0.1 wt.% BLG at pH=6.2.

This stability enhancement is probably related to the covalent disulfide bonds, which are known to form during heating between adsorbed BLG molecules [117] and between dissolved BLG molecules [119]. Our measurements showed that after heating, no desorption of protein is detected upon rinsing of the emulsions with electrolyte solution, which means that almost all molecules in the heated adsorption layer are irreversibly attached. Note that before heating, the BLG molecules adsorbed above the first layer were reversibly attached (see Section 6.1). Therefore, the results indicate that the heating leads to additional adsorption of protein and to formation of disulfide bonds between the adsorbed molecules, thus reinforcing the adsorption multilayer and enhancing the steric repulsion.

9.2.2. Effect of electrolyte concentration on the stability of heated emulsions

These experiments were performed with 0.1 wt.% BLG, at pH=6.2, and heating at 85 °C. One sees from Fig. 29 that the thermal treatment affects strongly the emulsion stability at high electrolyte concentrations only, $C_{EL} \geq 150$ mM, at which the electrostatic repulsion between the adsorbed protein molecules is suppressed (cf. with Fig. 23). We could speculate that the electrostatic repulsion between the adsorbed protein molecules at low and moderate electrolyte concentrations, C_{EL} of 1.5 mM and 10 mM, keeps these molecules separated from each other so that no intermolecular disulfide bonds are formed and, hence, the emulsion stability is not affected strongly upon heating.

9.2.3. Effect of pH on the stability of heated emulsions

These emulsions were prepared with solution of 0.1 wt.% BLG and C_{EL}=150 mM, and the heating was performed at 85 °C. One sees from Fig. 30 that emulsion stability significantly increases only when the thermal treatment is performed at pH>IEP≈5.0. When the thermal treatment is performed around the IEP, the stability of the heated and non-heated emulsions is almost the same. As explained in Section 6.3, the BLG adsorption around the IEP corresponds to a monolayer of more compact (less unfolded) molecules. We suppose that the reactive sulfhydryl and disulfide groups remain "hidden" in the interior of these compact molecules, which precludes formation of branched network of intermolecular S–S bonds upon heating. As a result, the layer structure and the emulsion stability do not change significantly after heating at/around the IEP of BLG (similar explanation was given in Ref. [122] to explain the pH dependence of the heat-induced gelling of BLG solutions).

9.2.4. Effect of heating of BLG emulsions on their long-term stability

This series of experiments was aimed to compare the short-term (3 h after preparation) and long-term stability (after 6 days of storage) of heated and non-heated emulsions. The experiments were performed with emulsions containing 0.1 wt.% BLG, and 1.5, 10 or 150 mM electrolyte, at heating temperature of 85 °C. As seen in Table 5, a moderate aging effect (30–40% decrease in emulsion stability) is observed at low electrolyte concentration, 1.5 and 10 mM, for the heated emulsions. In contrast, at high electrolyte concentration (150 mM) the coalescence stability of the heated emulsions does not change with the storage time. The latter result indicates that the conformational changes in the protein molecules occurring during heating at high C_{EL}, preclude the formation of non-covalent hydrogen and hydrophobic bonds, which cause the aging effect

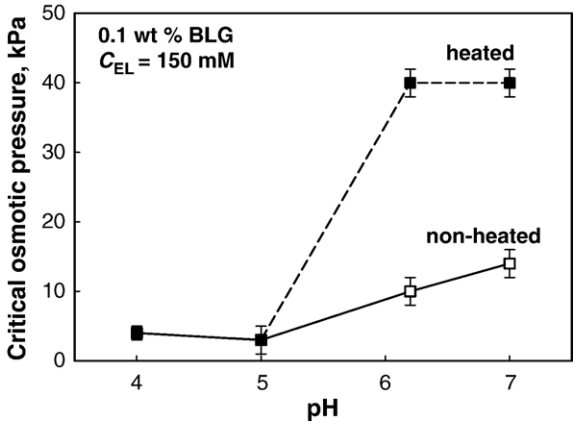

Fig. 30. Critical osmotic pressure as a function of pH for non-heated and heated at 85 °C emulsions, stabilized by 0.1 wt.% BLG at C_{EL}=150 mM.

Table 5
Critical osmotic pressure, P_{OSM}^{CR} [kPa], for heated and non-heated emulsions stabilized by 0.1 wt.% BLG, at three electrolyte concentrations, C_{EL} (pH=6.2)

C_{EL}, mM	Non-heated		Heated	
	3 h	6 days	3 h	6 days
1.5	6±1	5±1	8±2	5±2
10	13±2	9±2	13±2	10±2
150	10±1	3±0.5	40±4	40±4

described in Section 9.1. This hypothesis is supported by the FTIR spectra, which are presented and discussed in the following Section 9.3.

9.3. FTIR spectra

As discussed in Section 9.1, the pronounced aging effect observed at high electrolyte and protein concentrations (C_{EL}= 150 mM, C=0.1 wt.%), is not related to changes in the mean drop size or protein adsorption during emulsion storage. The results suggest that the aging is primarily caused by buildup of intralayer, non-covalent bonds between the adsorbed protein molecules. In contrast, the thermal treatment of BLG-emulsions significantly increases their stability and the aging effect disappears (see Table 5), which is explained by the formation of a network of denatured BLG molecules, cross-linked by S–S bonds.

The above explanations imply that the observed variations in the emulsion stability should be related to conformational changes in the adsorbed protein molecules. To check this hypothesis, we recorded FTIR spectra of protein solutions and emulsions (heated and non-heated, fresh, and aged) by following the procedure of Fang and Dalgleish [113].

9.3.1. Effects of storage time and heating on the FTIR spectra of BLG solutions

The FTIR spectra of heated and non-heated BLG solutions, stored for different periods of time, are compared in Fig. 31. From these spectra one can deduce that:

(1) The spectra of the fresh BLG solutions are similar to those reported in the literature, with six major characteristic bands at: 1694 cm^{-1} (β-type structure), 1680 cm^{-1} (β-sheet), 1668 cm^{-1} (β-turns), 1652 cm^{-1} (α-helix), 1634 and 1623 cm^{-1} (β-sheets) [113,122–124].
(2) The shelf-storage of non-heated solutions leads to significant changes in the spectra, which can be interpreted as a result of partial denaturing of the molecules, disintegration of protein aggregates present in the fresh solution (see the reduction of the peak at 1623 cm^{-1}), and formation of more hydrated, less compact protein structure — see the shifts of the β-sheet band from 1634 cm^{-1} to 1629 cm^{-1} and of the α-helix band from 1650 cm^{-1} to 1648 cm^{-1} [113,123].
(3) The heating of the protein solutions leads to strong local perturbation of the protein structure (the peaks are much wider and smaller in height; the respective spectrum is not shown in Fig. 31), but the original secondary structure of the dissolved protein remains stable upon long-term storage (see Fig. 31B).

9.3.2. Effects of protein adsorption and emulsion heating on the FTIR spectra

The comparison of the spectra obtained from non-heated BLG solution and from BLG-stabilized emulsion (several hours after emulsification) shows that the secondary structure of the BLG molecules remains well preserved for several hours after the adsorption — see the bands for β-sheets, β-turns and α-helix, which appear similar in the solutions and in the emulsions (cf. Figs. 31 and 32). This result is in agreement with the data of Fang and Dalgleish [113].

The BLG spectra obtained from freshly prepared and from 6-day stored (aged) emulsions are compared in Fig. 32. A large peak from disordered protein domains is seen at 1645 cm^{-1} in the spectrum of the aged emulsion, whereas this peak is almost missing for freshly adsorbed BLG. The decreased intensity of the β-sheet bands at 1637 and 1628 cm^{-1} is also related to increased fraction of the disordered domains — part of the initial β-sheets

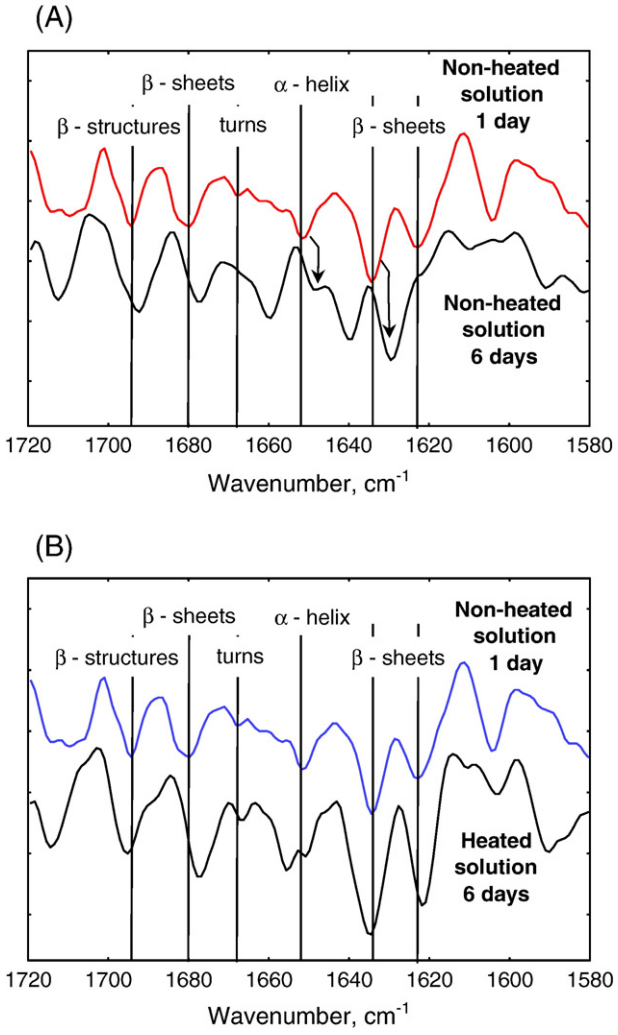

Fig. 31. Comparison of the FTIR spectra from BLG solutions: (A) non-heated, 1 day and 6 days after solution preparation; (B) fresh non-heated and heated (6 days after heating).

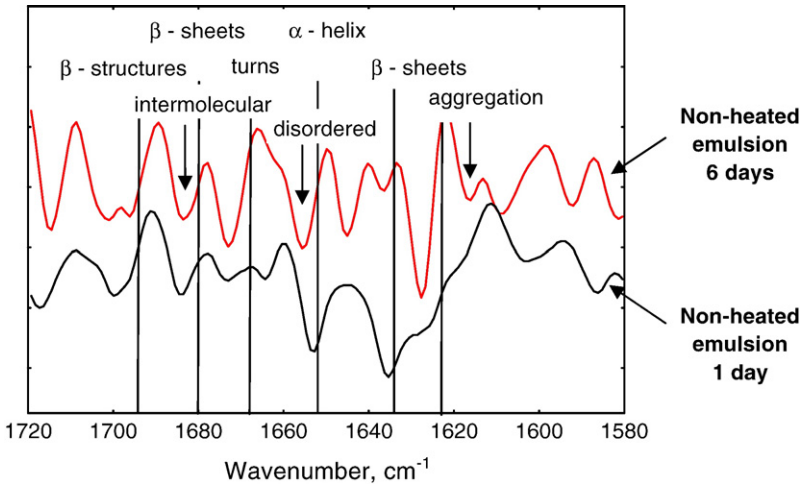

Fig. 32. Comparison of the FTIR spectra from non-heated BLG emulsions: 1 day and 6 days after emulsion preparation.

was probably transformed into disordered structure. New band appeared in the spectrum of the aged emulsion at 1616 cm^{-1}, which is attributed in the literature to formation of protein aggregates [124].

Let us compare now the spectra of 6-day stored emulsion and 6-day stored BLG solution (cf. Figs. 31A and 32). This comparison allows one to reveal the conformational changes after storage, which are related to protein adsorption. The main difference between the spectra of aged emulsion and aged solution could be summarized as follows: In the spectrum of the aged emulsion we see bands at 1684 cm^{-1} and 1616 cm^{-1} from intermolecular bonds, and band at 1645 cm^{-1} from disordered structures, which are missing in the spectrum of the aged BLG solution. Hence, the emulsion storage leads to enhanced disordering of the adsorbed protein molecules and to formation of intermolecular bonds (these two processes are probably interrelated). One could expect that the observed decrease in emulsion stability after shelf-storage is closely related to the conformational changes in the adsorbed molecules, detected by the FTIR spectra.

Fig. 33 compares the FTIR spectra of heated emulsion after 6 days of storage and of fresh BLG solution. Interestingly, the main bands related to the β-sheets at 1694 cm^{-1}, 1680 cm^{-1}, 1634 cm^{-1} and 1623 cm^{-1} remained almost the same in intensity and width, which indicates that the secondary structure of the protein in heated emulsion is very well preserved during shelf-storage, which correlates with the preserved emulsion stability (the aging effect disappears after emulsion heating).

Let us compare now the spectra of heated and non-heated emulsions, which had been stored for 6 days (cf. Figs. 32 and 33). The main β-structure bands remained almost the same in the heated emulsion after storage. In contrast, the protein in the non-heated emulsion significantly changed its secondary structure during storage, and many disordered regions and intermolecular bonds were formed. These differences in the spectra of the two emulsions correlate with the observed differences in emulsion stability — large aging effect for the non-heated emulsions and no aging effect for the heated ones (see the bottom line of Table 5).

In conclusion, no significant difference is observed between the spectra of heated and non-heated emulsions within several hours after their preparation. However, after 6 days of storage, the secondary structure of the adsorbed protein in heated emulsion remained almost the same as that of the initially dissolved protein, whereas the adsorbed molecules in the non-heated emulsion significantly changed their structure — more disordered structure and surface aggregates were formed. These conformational changes correlate well with the changes in emulsion stability observed after heating and shelf-storage.

10. Comparison of β-lactoglobulin and whey protein concentrate (WPC) as emulsifiers

Since BLG is the major component of whey protein concentrate (WPC), one could expect similar properties of the emulsions stabilized by these two protein samples. To check this expectation, we performed comparative experiments with emulsions stabilized by WPC and BLG — see Table 6 for summary of the main results.

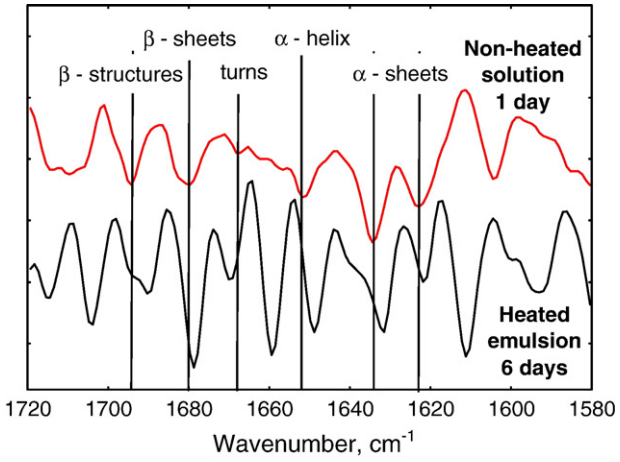

Fig. 33. Comparison of the FTIR spectra from heated BLG emulsion (6 days after heating) and fresh non-heated BLG solution.

Table 6
Comparison of the properties of BLG and WPC as emulsifiers, 150 mM NaCl

Property	BLG		WPC	
	Native lyophilized (freeze dried)		Heated during spray-drying	
Adsorption	$C_{SER}<0.03$ wt.% Monolayer with $\Gamma\approx 1.5$ mg/m^2 $\Gamma_M\approx 1.65$ mg/m^2	$C_{SER}>0.03$ wt.% Multilayer	$C_{SER}<0.1$ wt.% Monolayer with $\Gamma\approx 1.9$ mg/m^2 $\Gamma_M\approx 2.0$ mg/m^2	$C_{SER}>0.1$ wt.% Multilayer
Dependence of coalescence stability on Γ	Unstable at $\Gamma/\Gamma_M<0.9$ Rapid increase at $\Gamma/\Gamma_M\approx 0.9$ Gradual increase at higher Γ			
Decrease of stability after aging (6 days)	~30%	~3 times	No effect	
Stability increase after heating	~40%	~4 times	<10%	
Effect of pH on stability	~3 times decrease when pH changes from 6.2 to 5.0		No effect when pH varies in the range between 6.2 and 4.0	

For both protein samples, at high electrolyte concentration and natural pH, we found well-defined protein concentration which separates the adsorption in a monolayer from the adsorption in a multiplayer, $C_{TR}^{INI}=0.03$ wt.% for BLG and 0.1 wt.% for WPC in the experiments performed by us [36,45] (note that the particular value of C_{TR}^{INI} depends on the oil volume fraction and drop size, as seen from Eq. (10)).

The adsorption in the completed protein monolayer is different: $\Gamma_M\approx 1.65$ mg/m^2 for BLG and 2.0 mg/m^2 for WPC. As explained in Section 6.1, the maximal possible adsorption in a dense monolayer of intact BLG molecules is $\Gamma_{Int}\approx 2.75$ mg/m^2. The comparison between Γ_M for BLG and Γ_{Int} shows that the protein unfolding after adsorption leads to about 40% increase in the average area per BLG molecule. Assuming that the adsorption layer of WPC consists mainly of BLG molecules, the value of $\Gamma_M\approx 2.0$ mg/m^2 indicates somewhat smaller increase of the area per molecule upon adsorption, ≈27%, in WPC-stabilized emulsions (i.e., the adsorbed molecules are more compact).

Very significant differences between BLG and WPC were found for the effects of various factors on emulsion stability: the stability of WPC-containing emulsions did not change after thermal treatment [36], no emulsion aging was observed, and the effect of pH was relatively small (Table 6). All these results show that the protein molecules in the studied WPC sample are much more robust and do not change upon variation of the conditions. The latter conclusion can be explained by the fact that the used WPC sample is produced by spray-drying procedure, which includes heating of the protein at high temperature (in contrast to BLG, which is produced by freeze-drying). The thermal treatment during the WPC production probably led to a partial denaturing of the protein molecules and to formation of strong intramolecular bonds, which fixed the structure of the protein molecules (some intermolecular bonds were also formed, which was evident from the presence of many aggregates in the WPC used [7]). In a first approximation, one can consider the protein molecules in the studied WPC sample as relatively stable "balls", which do not form extensive intermolecular bonds after adsorption, heating or changing pH, which is in sharp contrast to the molecules in the BLG sample studied.

The above explanation was supported by control experiments performed with mixture of the main protein components of WPC (57 wt.% BLG, 37 wt.% αLA, and 6 wt.% BSA). This mixture, called "WPC-mimic", was prepared with freeze-dried proteins only. We found that the emulsifying properties of WPC-mimic were very similar to the properties of BLG. Therefore, one could not explain the observed differences between the WPC and BLG samples (Table 6) by their different protein compositions.

11. Discussion of the mechanisms of emulsion stabilization by globular proteins

In this section we summarize the main conclusions for the coalescence stability of the studied emulsions and, on this basis, discuss the possible mechanisms of film rupture upon compression and/or sliding of neighboring emulsion drops. Note that the external forces, such as gravity, hydrodynamic forces, and centrifugal forces have two components: (1) normal component with respect to the line of drop-centers, which leads to the formation of planar emulsion film between compressed drops, and acts as to squeeze the liquid from this film against the disjoining pressure barrier; (2) tangential component, which creates a tangential stress able to tear the protein adsorption layers thus creating bare spots in the film, which are not protected by protein. Both components can rupture the films and cause drop coalescence.

The obtained experimental results allow us to distinguish three types of emulsion stabilization:

11.1. Electrostatically stabilized emulsions

At pH > 6.0 and low electrolyte concentrations, $C_{EL}\le 50$ mM (Fig. 23), the protein molecules are charged, which leads to electrostatic repulsion between the neighboring protein molecules inside the adsorption layers, as well as between the adsorption layers on two neighboring emulsion drops. This electrostatic repulsion keeps the adsorbed protein molecules at a certain distance from each other and hampers the formation of both non-covalent and covalent bonds within the adsorption layer. Therefore, the stability of such emulsions is governed mainly by long-ranged electrostatic and van der Waals forces. The most important factors are the electrolyte concentration and pH, which govern the electrostatic repulsion. The structure of the

adsorption layers and the emulsion stability do not change significantly after heating and with storage time.

On the basis of this molecular picture, we can propose a possible mechanism of rupture of the emulsion films in the electrostatically-stabilized emulsions (see Fig. 34). When the drop surfaces are pushed against each other, the electrostatic repulsion between the adsorption layers creates a barrier, which resists thinning of the emulsion film. If the compressing pressure is higher than this barrier, the latter is overcome and the film spontaneously thins until the adsorption layers on the two opposite film surfaces come in contact with each other. Since the electrostatic repulsion is relatively "soft", the protein molecules can rearrange and possibly form a bridging monolayer between the two surfaces of the emulsion film (see Fig. 34B) (such a process was observed by optical microscopy in the experiments with latex particles [125,126]). Furthermore, the bridging monolayer of uniformly spaced molecules depicted in Fig. 34B is inherently unstable, due to lateral capillary forces (which lead to lateral attraction between the neighboring protein molecules in the film [107,127–129]) and to strong van der Waals forces between the two film surfaces, separated by only a few nanometers. Therefore, a spot deprived of protein molecules could spontaneously form and expand with time in the emulsion film, leading to direct contact of the two opposite oil–water interfaces, with a subsequent rupture of the film and drop coalescence.

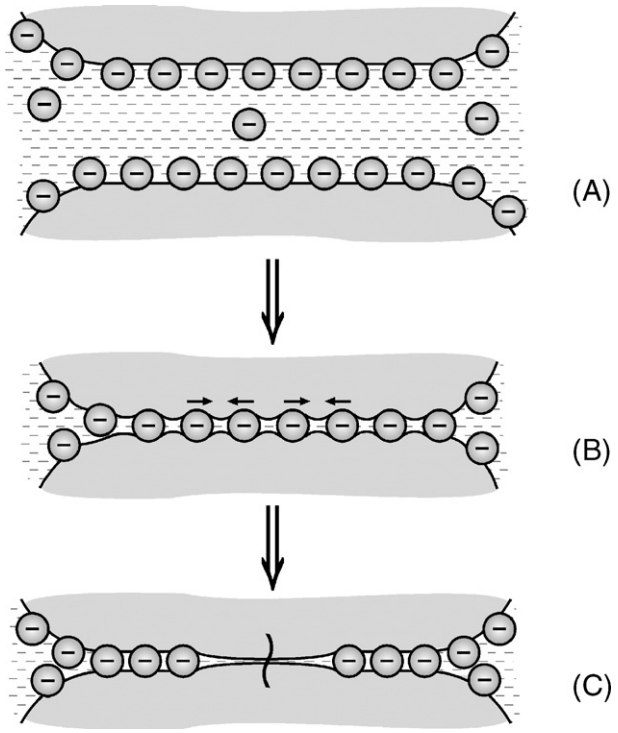

Fig. 34. Schematic presentation of a hypothetical mechanism of emulsion film rupture in electrostatically stabilized emulsions. (A, B) After the electrostatic barrier is overcome, the two film surfaces spontaneously thin down and a bridging monolayer of protein molecules can be formed. (C) This bridging monolayer is unstable, because lateral capillary forces between the protein molecules and the van der Waals interaction between the two oil–water interfaces would act so as to create bare thin spots in the film, unprotected by protein molecules. The film rupture is schematically shown in (C) by vertical wavy line (see Section 11 for further explanations). For clarity, the positively charged counterions are not shown.

11.2. Emulsions stabilized by steric repulsion between adsorption monolayers

Such type of emulsion stabilization occurs at low protein concentration and: (1) at all studied electrolyte concentrations, if pH ≈ IEP, (2) at high electrolyte concentrations ($C_{EL} \geq 150$ mM), if pH ≥ 6.2 (see Fig. 23). Under these conditions, the electrostatic repulsion between the protein molecules is negligible, due to their small net charge and/or to the repulsion screening by electrolyte. The emulsion stability is determined by steric repulsion between adsorption monolayers on the surfaces of two neighboring drops, which touch each other. The stability of these emulsions depends mainly on pH (which governs the conformation of the adsorbed molecules) and on protein concentration (which governs the amount of adsorbed protein). The storage time and heating have an intermediate effect, whereas the electrolyte concentration has a small effect on emulsion stability in these systems (see Fig. 22).

One may expect that in these systems, the emulsion film rupture and drop coalescence occur after expansion of the drop surface (as a result of drop deformation or thermal fluctuations of the film surface) and/or upon application of tangential stress to the film surface (e.g., in sheared emulsions), which break the continuous adsorption layers and create "bare" spots deprived of protein molecules (see Fig. 1B). This picture of film rupture suggests that the stability of such emulsions should be related to the rheological properties of the adsorption layers, such as yield stress or yield strain, mechanical elasticity, etc. In turn, these properties depend mostly on the conformational state of the adsorbed protein molecules and on the intermolecular bonds between them [130–132].

11.3. Emulsions stabilized by steric repulsion between protein adsorption multilayers

Steric stabilization due to overlapping multilayers occurs at high electrolyte and protein concentrations ($C_{EL} \geq 100$ mM, $C_{PR} \geq 0.1$ wt.%) and pH ≥ 6.2. The key factors here are the protein concentration, and the type and strength of intermolecular bonds. Non-covalent bonds are formed upon shelf-storage and lead to gradual decrease of emulsion stability with time (for non-heated emulsions). In contrast, the emulsion heating leads to formation of covalent S–S bonds between the adsorbed molecules, thus reinforcing the adsorption layers and increasing emulsion stability. Also, the heating preserves the structure of the protein molecules and the aging effect disappears.

The following molecular mechanism of emulsion film rupture could be proposed for these systems. The films are primarily stabilized through steric repulsion, created by overlapping adsorption multilayers. As seen from Fig. 22, the steric repulsion created by protein monolayers, obtained at the same pH and ionic strength (but at lower protein concentration), provides a lower barrier to coalescence in comparison with the barrier created by multilayers. Therefore, once the steric barrier created by the multilayers is overcome (due to drop

compression or emulsion shear), one may expect an almost immediate film collapse and drop coalescence, because the secondary barrier created by the monolayers is lower and cannot ensure film stability.

12. Comparison of emulsion coalescence and flocculation stabilities

A detailed experimental study of drop flocculation in BLG-stabilized emulsions was preformed by McClements and coworkers [22,133–140], and Kulmyrzaev and Schubert [37]. The effects on the mean-floc-size of electrolyte concentration, pH, thermal treatment and storage time were experimentally evaluated [22,37,133–140] and the main conclusions from these studies could be summarized as follows:

(1) The flocculation strongly increases at high electrolyte concentrations, due to suppressed electrostatic repulsion between the drops [22].
(2) Strong flocculation is observed at pH around the isoelectric point (IEP) [37]. No significant effect of the electrolyte is observed around the IEP, because the electrostatic interactions are of secondary importance [37].
(3) The emulsion heating at neutral pH, in presence of 150 mM NaCl, leads to significant flocculation, which is explained by the formation of intermolecular S–S bonds between the adsorption layers of two neighboring drops [135].
(4) The emulsion heating at neutral pH = 7 does not affect the flocculation stability at low ionic strength [22,135]. This result is explained by the formation of intramolecular S–S bonds, which do not lead to flocculation. Intermolecular S–S bonds between neighboring drops are not formed, due to electrostatic repulsion, which keeps the drops separated from each other [22,135].
(5) The heating at pH = 3 has no significant effect. This result is explained by the stable conformation of the BLG molecules at low pH, which precludes molecule unfolding and formation of intermolecular S–S bonds [140].

Let us compare briefly the coalescence and flocculation stabilities of BLG emulsions: One sees from Table 7 a good agreement between the trends in the flocculation and coalescence stabilities for the electrostatically-stabilized emulsions. In these emulsions, the average floc-size (which is a measure of emulsion flocculation stability) and the critical osmotic pressure (which is a measure of coalescence stability) remain almost constant with storage time and after heating, which is explained by the significant electrostatic repulsion between the adsorbed molecules. This repulsion presumably keeps the molecules separated from each other, and does not allow the formation of strong intermolecular bonds within the adsorption layers and between the adsorption layers of two neighboring drops.

When the emulsions are stabilized by steric repulsion from adsorption multilayers (high protein and electrolyte concentrations), both the flocculation [138,139] and coalescence stabilities are affected significantly by the storage time and heating. Interestingly, the emulsion heating and aging lead to larger flocs, indicating *decreased* flocculation stability [138,139], whereas the coalescence stability *increases* after heating and decreases with storage time [36]. These results are explained by the different types of bonds formed during heating and upon storage. As suggested in Section 9 and discussed in Ref. [36], non-covalent bonds are formed during storage, whereas S–S bonds are formed after heating. The experimental results show that both types of bonds enhance flocculation, whereas only the S–S bonds increase the coalescence stability.

For the emulsions stabilized by protein monolayers (low protein concentration and high electrolyte concentration) we also see similar trends when comparing the flocculation and coalescence stabilities. Both the flocculation and coalescence stabilities are lower, in comparison with the emulsions stabilized by multilayers, at the same pH and ionic strength, which is probably due to weaker steric repulsion and to possible presence of hydrophobic attraction [138,139,39]. Upon shelf-storage and heating, only slight changes in flocculation and coalescence stabilities are observed.

13. Summary and conclusions

In this review we summarize our recent results about the coalescence in emulsions stabilized by globular milk proteins. The major aims of these studies were to clarify the effects of various factors on emulsion coalescence stability and the mechanisms of emulsion stabilization by proteins. To achieve these aims we used a combination of several experimental methods, which provided useful complementary information: (1) centrifugation for quantification of coalescence stability; (2) the methods of Bradford and BCA for determination of protein adsorption in batch emulsions; (3) Film Trapping Technique to quantify the effect of drop size on coalescence stability; (4) FTIR for investigation of the conformational changes and bond formation in the protein adsorption layers. In addition, experiments with narrow gap homogenizer were performed to clarify the role

Table 7
Qualitative comparison of the effects of aging and heating on the flocculation and coalescence stabilities of BLG emulsions at pH between 6 and 7 (see also Fig. 23)

Type of emulsion stabilization	Conditions	Storage time up to 6 days		Heating	
		Coalescence stability	Flocculation stability	Coalescence stability	Flocculation stability
Electrostatic	C_{EL} < 50 mM arbitrary C_{BLG}	Slight effect	No effect	No effect	
Steric by adsorption monolayers	$C_{EL} \geq 150$ mM low C_{BLG}	~30% decrease	Rapid decrease; no change afterwards	Slight increase	Slight decrease
Steric by adsorption multilayers	$C_{EL} \geq 150$ mM high C_{BLG}	Significant decrease after ~1 day		Strong increase	Strong decrease

of drop-drop coalescence during emulsification in a turbulent flow.

The main experimental results and conclusions could be summarized as follows:

13.1. Coalescence during emulsification (Section 3)

1. Two regimes of emulsification (surfactant-rich and surfactant-poor) are observed in all studied systems. The effect of drop coalescence on the mean drop size, d_{32}, is negligible in the surfactant-rich regime, whereas the coalescence plays an important role in the surfactant-poor regime.
2. In the surfactant-rich regime, d_{32} does not depend on emulsifier concentration and is determined mainly by the interfacial tension, oil viscosity (see also Refs. [73–78]), and power dissipation density, ε, in the emulsification chamber (see Eq. (7)).
3. In the surfactant-poor regime and suppressed electrostatic repulsion, d_{32} is a linear function of the initial emulsifier concentration, $1/C_{INI}$. From the line slope, one can determine the threshold emulsifier adsorption, Γ^*, needed to stabilize the drops during emulsification. Γ^* is a characteristic of the emulsifier used, because it does not depend on the oil volume fraction and power dissipation density, ε. During shelf-storage, these emulsions remain stable.
4. In the surfactant-poor regime and significant electrostatic repulsion, the emulsifier adsorption strongly depends on emulsification conditions. The emulsions obtained are unstable upon shelf-storage, because the adsorption after emulsification is insufficient to protect the drops against coalescence.

13.2. Mode of coalescence upon shelf-storage and during centrifugation (Sections 4 and 5)

1. A theoretical analysis shows that two different in size emulsion films are formed in the uppermost layer of the emulsion column in contact with a continuous layer of oil: emulsion films between two drops and films between a drop and a large oil–water interface. By considering the roles of the film size and of the capillary pressure of the drops in the coalescence process, we showed that two modes of emulsion destabilization could be expected. This theoretical prediction was experimentally verified with emulsions stabilized by BLG of different concentrations.
2. A new experimental procedure is proposed which allows one to determine the dependence of the emulsion osmotic pressure on the drop volume fraction $P_{OSM}(\Phi)$ by centrifugation.

13.3. Protein adsorption on drop surface for BLG containing emulsions (Section 6)

1. At low electrolyte concentration, the protein adsorbs in a monolayer. If the pH is away from the protein isoelectric point (IEP), the adsorbed molecules are probably separated apart from each other, which precludes formation of strong intermolecular bonds during shelf-storage and after heating.
2. At higher electrolyte concentration, the adsorption Γ increases, as a result of suppressed electrostatic repulsion between the protein molecules. Protein monolayer or multilayer is formed depending on the protein concentration and pH (see Fig. 19).
3. Protein adsorption passes through a maximum (situated around the isoelectric point, IEP), as a function of pH (Fig. 20). This maximum is explained by the suppressed electrostatic repulsion between the protein molecules.

13.4. Short-term stability of BLG containing emulsions (Sections 7 and 8)

1. Emulsion stability increases in a step-wise manner with the protein adsorption, Γ (Fig. 21B). At high electrolyte concentration, almost complete adsorption monolayer is required to obtain stable emulsion.
2. If the pH is away from the IEP and $C_{EL} < 100$ mM, the coalescence stability is governed mainly by electrostatic and van der Waals forces (DLVO-type of stabilization).
3. If the protein adsorbs as a multiplayer (high electrolyte and protein concentrations), one should take into account the contribution of the steric repulsion, along with the DLVO forces.
4. If the protein adsorption corresponds to a monolayer, Γ_M, and the electrostatic repulsion is suppressed ($C_{EL} > 100$ mM), the emulsion stability does not depend significantly on electrolyte concentration, but depends on pH.
5. The stability of BLG emulsions is very low at pH ≈ IEP, although the protein adsorption is highest there.
6. The emulsions containing larger drops are less stable under all other equivalent conditions.
7. The heating of BLG emulsions, prepared at high electrolyte and protein concentrations (multilayer adsorption), increases the short-term emulsion stability which is explained by the formation of a network of BLG molecules, cross-linked by disulfide bonds. In contrast, the heating of emulsions containing electrolyte of low and moderate concentration ($\leq$ 10 mM) does not affect significantly the emulsion coalescence stability.

13.5. Long-term stability and aging of BLG containing emulsions at high electrolyte and protein concentrations (multilayer adsorption)

1. The stability of BLG-containing emulsions significantly decreases after one day of shelf-storage. This phenomenon is termed “the aging effect” and is not related to changes in the mean drop size or protein adsorption.
2. The aging effect is caused by conformational changes in the protein adsorption layer, accompanied by formation of non-covalent bonds (H-bonds and hydrophobic interactions) between the adsorbed molecules. Probably, these bonds transform the adsorption layer into a fragile/brittle shell, which is inefficient in protecting the drops against coalescence.
3. The FTIR spectra show that the heating preserves the initial conformation of the adsorbed BLG molecules upon shelf-

storage, which correlates very well with the disappearance of the aging effect after heating.

4. Parallel experiments with whey-protein concentrate (WPC) stabilized emulsions showed that these are less sensitive to variations of pH and thermal treatment. No aging effect is detected for these emulsions. In all other aspects, there is a close similarity between the BLG and WPC-stabilized emulsions. The observed differences between BLG and WPC are explained with the different procedures for preparation of these protein samples (freeze-drying and thermally enhanced spray-drying, respectively).

An important conclusion from this study is the establishment of three different types of emulsion stabilization (see Fig. 23): (1) electrostatically stabilized emulsions with monolayer adsorption; (2) emulsions stabilized by steric repulsion, created by protein adsorption multilayers; and (3) emulsions stabilized by steric repulsion, created by adsorption monolayers. The coalescence stability of emulsions of type 1 can be reasonably well described by the DLVO theory. The stability of emulsions of type 2 is described by a simple model, which accounts for the steric +DLVO interactions. Further experimental and theoretical efforts are needed to reveal the main factors which determine the stability of emulsions of type 3.

14. Abbreviations and notation

Abbreviations

αLA	α-lactalbumin
BCA	Bicinchoninic acid, Ref. [141]
BLG	β-lactoglobulin
BSA	bovine serum albumin
Brij 58	hexadecylpolyoxyethylene-20 (nonionic surfactant)
DTT	dithiothreitol
IEP	isoelectric point of protein
fcc	face-centered-cubic lattice
FTIR	Fourier transform infra-red spectroscopy, Section 2.6
FTT	film trapping technique, Section 2.5.1
SBO	soybean oil
SDS	sodium dodecyl sulfate
WPC	whey protein concentrate

Notation

Capital Roman letters

A — area
- A_{TT} — cross-sectional area of the test tube, Eq. (3)
- A_W — area of the wetting film between drop in the 1st emulsion layer and solid wall, Fig. 12A
- A_D — area of the emulsion film between two drops, Fig. 12
- A_{OI} — area of the film between drop in the 1st emulsion layer and continuous oil layer, Fig. 12B

A_H — Hamaker constant
- A_{ijk} — Hamaker constant for interaction of phase i with phase k through phase j

C — concentration
- C_{INI} — initial protein or surfactant concentration in the aqueous phase before emulsification
- C_{SER} — protein or surfactant concentration in the serum after emulsification
- $\Delta C=(C_{INI}-C_{SER})$
- C_{TR} — initial emulsifier concentration at which the transition between the surfactant-poor and the surfactant-rich regimes occurs, Eq. (11)

C_{EL} — electrolyte concentration

F — force
- F_W — repulsive force between solid wall and a drop in 1st emulsion layer, Fig. 12
- F_D — vertical projection of the force, exerted on drop in the 1st emulsion layer from its neighbors in the second layer of drops, Fig. 12

H — height
- H_{OIL} — height, which the oil in an emulsion would have (placed in a test tube with cross-sectional area A_{TT}), if the oil were completely separated, Eq. (26)
- H_K — equilibrium height of the emulsion cream in centrifugal test tube, at given acceleration, g_k, Fig. 4A
- H_{REL} — height of the released oil on top of the cream after centrifugation, Fig. 4
- $\tilde{H}_K$ — dimensionless height of the emulsion cream at acceleration g_K, Eq. (28)

L — characteristic length of steric repulsion, Eq. (38)

P — pressure
- P_A — air pressure in the capillary of the FTT set-up, Fig. 3
- P_{A0} — atmospheric pressure, Fig. 3
- P_C — capillary pressure
- P_C^{CR} — critical capillary pressure leading to coalescence of an oil drop with large oil phase in the FTT experiments, Fig. 3C
- P_{OI} — pressure in the curved film between drop in the 1st emulsion layer and the bulk oil phase, Eq. (16)
- P_D — pressure of the oil inside a drop, Fig. 4
- P_{CAP} — capillary pressure of an oil drop
- P_{OSM} — osmotic pressure of concentrated emulsion, Fig. 4
- $\tilde{P}_{OSM}$ — dimensionless osmotic pressure, Eq. (23)
- P_{OSM}^{CR} — critical osmotic pressure for coalescence, Eq. (3)
- P_W — pressure of water inside the Plateau borders of concentrated emulsion, Fig. 4
- P_{OIL} — pressure of the oil which is released as continuous layer on top of the emulsion cream, Fig. 4
- P_T — fluctuations of the hydrodynamic pressure in turbulent flow, Eq. (4)

R — radius
- R_F — radius of curvature of emulsion film in FTT experiments, Eq. (16)
- R_0 — radius of non-deformed drop
- R_{32} — mean volume-surface radius ($R_{32}=d_{32}/2$)

T — temperature

V — volume
- V_{OIL} — total volume of oil in the emulsion
- V_C — volume of the aqueous phase in the emulsion
- V_{REL} — volume of released oil on top of the emulsion cream after centrifugation, Eq. (3)

V_D — drop volume

Small Roman letters

a — capillary length in gravity field
a_k — capillary length in centrifugal field with relative acceleration k
d — diameter
d_{32} — mean volume-surface diameter, Eq. (1)
d_K — Kolmogorov size, Eq. (7)
$f(\Phi)$ — fraction of the interface between an emulsion and continuous oil phase which is occupied by emulsion films, Eq. (25)
f^{TR} — threshold value of $f(\Phi)$ separating the two modes of coalescence (drop-drop and drop-large phase), Eq. (22)
g — gravitational acceleration
g_k — centrifugal acceleration
h — film thickness, Fig. 2
k_B — Boltzmann constant
$k=g_K/g$ — relative centrifugal acceleration,
m — number of close neighbors located in the second emulsion layer, Eq. (14)
n_0 —number concentration of electrolyte
t — time

Capital Greek letters

Φ — oil volume fraction
Γ — adsorption
Γ^* — threshold emulsifier adsorption needed to stabilize drops against coalescence during emulsification
Γ_M — adsorption in dense monolayer
Γ_T — number density of protein aggregates (polymer chains) per unit area of the adsorption layer, Eq. (38)
Π — disjoining pressure
Π_{MAX} — maximum of the disjoining pressure isotherm, Fig. 1
Π_{OI} — disjoining pressure of the curved film between a drop in the 1st emulsion layer and bulk oil phase, Eq. (16)
Π_D — disjoining pressure of the film between two emulsion drops, Section 4
Π_{EL} — electrostatic component of the disjoining pressure, Eq. (36)
Π_{VdW} — van der Waals component of the disjoining pressure, Eq. (35)
Ψ_S — electrical surface potential of the drops

Small Greek letters

δ — thickness of protein adsorption layer
ε — rate of energy dissipation per unit mass in turbulent flow [J/kg s]
η — viscosity
η_O — oil viscosity
κ — inverse Debye screening length, Eq. (36)
ρ — mass density
ρ_D — of the dispersed phase
ρ_C — of the continuous phase
$\Delta\rho=(\rho_C-\rho_D)$
σ_{OW} — oil–water interfacial tension

Acknowledgement

The studies reviewed in this paper are supported by Kraft Foods, Glenview, IL. Useful discussions with Dr. C. Oleksiak and Dr. R. Borwankar (Kraft Foods), and with Dr. K. Marinova (Sofia University) are gratefully acknowledged. The FTIR spectra were kindly recorded and processed by Prof. B. Yordanov and his colleagues from the Bulgarian Academy of Sciences. Some emulsification experiments and centrifugation tests were performed by Dr. D. Sidjakova, and her help is highly appreciated.

References

[1] Das KP, Kinsella JE. Stability of food emulsions: physicochemical role of protein and nonprotein emulsifiers. Adv Food Nutr Res 1990;34:81.
[2] Dickinson E. Proteins at interfaces and in emulsions. Stability, rheology and interactions. J Chem Soc Faraday Trans 1998;94:1657.
[3] Walstra P, Geurts TJ, Noomen A, Jellema A, van Boekel AAJS. Dairy Technology. New York: Marcel Dekker; 1999.
[4] Walstra P. Formation of emulsions. In: Becher P, editor. Encyclopedia of Emulsion Technology. New York: Marcel Dekker; 1983. Chapter 2.
[5] Walstra P, Smulders P. Formation of emulsions. Proceedings of the 1st World Congress on Emulsions. France: Paris; 1993.
[6] Walstra P, Smulders I. Making emulsions and foams: an overview. In: Dickinson E, Bergenstühl B, editors. Food Colloids: Proteins, Lipids and Polysaccharides. Procs. Int. Symp. Royal Soc. of Chem. Cambridge; 1997. p. 367–81.
[7] Tcholakova S, Denkov ND, Sidzhakova D, Ivanov IB, Campbell B. Interrelation between drop size and protein adsorption at various emulsification conditions. Langmuir 2003;19:5640.
[8] Tcholakova S, Denkov ND, Danner T. Role of surfactant type and concentration for the mean drop size during emulsification in turbulent flow. Langmuir 2004;20:7444.
[9] Graham DE, Phillips MC. Proteins at liquid interfaces: I. Kinetics of adsorption and surface denaturation. J Colloid Interface Sci 1979;70:403.
[10] Graham DE, Phillips MC. Proteins at liquid interfaces: II. Adsorption isotherms. J Colloid Interface Sci 1979;70:415.
[11] Graham DE, Phillips MC. Proteins at liquid interfaces: III. Molecular structure of adsorbed films. J Colloid Interface Sci 1979;70:427.
[12] Graham DE, Phillips MC. Proteins at liquid interfaces: IV. Dilatational properties. J Colloid Interface Sci 1980;76:227.
[13] Graham DE, Phillips MC. Proteins at liquid interfaces: V. Shear properties. J Colloid Interface Sci 1980;76:240.
[14] Atkinson PJ, Dickinson E, Horne DS, Richardson R. Neutron reflectivity of adsorbed b-casein and b-lactoglobulin at the air/water interface. J Chem Soc Faraday Trans 1995;91:2847.
[15] Beverung CJ, Radke CJ, Blanch HW. Protein adsorption at oil/water interface: characterization of adsorption kinetics by dynamic interfacial tension measurements. Biophys Chemist 1999;81:59.
[16] Benjamins J. Static and dynamic properties of proteins adsorbed at liquid interfaces, PhD Thesis, Wageningen University, 2000.
[17] Oberholzer MR, Lenhoff AM. Protein adsorption isotherms through colloidal energetics. Langmuir 1999;15:3905.
[18] Makievski AV, Loglio G, Kragel J, Miller R, Fainerman VB, Neumann AW. Adsorption of protein layers at the water/air interface as studied by axisymmetric drop and bubble shape analysis. J Phys Chem B 1999;103:9557.
[19] Miller R, Fainerman VB, Makievski AV, Kragel J, Grigoriev DO, Kazakov VN, et al. Dynamics of protein and mixed protein/surfactant adsorption layers at the water/fluid interface. Adv Colloid Interface Sci 2000;86:39.
[20] Pugnaloni LA, Dickinson E, Ettelaie R, Mackie AR, Wilde PJ. Competitive adsorption of proteins and low-molecular-weight surfactants: computer simulation and microscopic imaging. Adv Colloid Interface Sci 2000;86:39.

[21] Euston SR. Computer simulation of proteins: adsorption, gelation and self-association. Curr Opin Colloid Interface Sci 2004;9:321.
[22] McClements DJ. Protein-stabilized emulsions. Curr Opin Colloid Interface Sci 2004;9:305.
[23] Van Aken GA, Blijdenstein TBJ, Hotrum NE. Colloidal destabilisation mechanisms in protein-stabilised emulsions. Curr Opin Colloid Interface Sci 2003;8:371.
[24] Dimitrova TD, Gurkov TD, Vassileva ND, Campbell BE, Borwankar RP. Kinetics of cream formation by the mechanism of consolidation in flocculating emulsions. J Colloid Interface Sci 2000;230:254.
[25] Dickinson E, Golding M, Povey MJW. Creaming and flocculation of oil-in-water emulsions containing sodium caseinate. J Colloid Interface Sci 1997;185: 515.
[26] Dickinson E, Ritzoulis C, Povey MJW. Stability of emulsions containing both sodium caseinate and Tween 20. J Colloid Interface Sci 1999;212: 466.
[27] Dalgleish DG. Food emulsions stabilized by proteins. Curr Opin Colloid Interface Sci 1997;2:573.
[28] Izmailova VN, Yampolskaya GP. Rheological parameters of protein interfacial layers as a criterion of the transition from stable emulsions to microemulsions. Adv Colloid Interface Sci 2000;88:99.
[29] Graham DE, Phillips MC. The conformation of proteins at interfaces and their role in stabilizing emulsions. In: Smith AL, editor. Theory and Practice of Emulsion Technology. New York: Academic Press; 1976. p. 75.
[30] Phillips MC. Protein conformation at liquid interfaces and its role in stabilizing emulsions and foams. Food Technol 1981;1:50.
[31] Martin A, Bos M, Stuart MC, van Vliet T. Stress–strain curves of adsorbed protein layers at the air/water interface measured with surface shear rheology. Langmuir 2002;18:1238.
[32] Murray B. Interfacial rheology of food emulsifiers and proteins. Curr Opin Colloid Interface Sci 2002;7:426.
[33] Petkov JT, Gurkov TD, Campbell B, Borwankar RP. Dilatational and shear elasticity of gel-like protein layers on air–water interface. Langmuir 2000;16:3703.
[34] Murray BS, Cattin B, Schuler E, Sonmez ZO. Response of adsorbed protein films to rapid expansion. Langmuir 2002;18:9476.
[35] Roth S, Murray BS, Dickinson E. Interfacial shear rheology of aged and heat-treated b-lactoglobulin films: displacement by nonionic surfactant. J Agric Food Chem 2000;48:1491.
[36] Tcholakova S, Denkov ND, Ivanov IB, Campbell B. Coalescence in protein stabilized emulsions, Paper included in the Proceedings of the Third World Congress on Emulsions, Lyon 2002, Paper No 200.
[37] Kulmyrzaev AA, Schubert H. Influence of KCl on the physicochemical properties of whey protein stabilized emulsions. Food Hydrocol 2004;18: 13.
[38] Narsimhan G. Maximum disjoining pressure in protein stabilized concentrated oil-in-water emulsions. Colloids Surf 1992;62:41.
[39] Tcholakova S, Denkov ND, Sidzhakova D, Ivanov IB, Campbell B. Effects of electrolyte concentration and pH on the coalescence stability of b-lactoglobulin emulsions: experiment and interpretation. Langmuir 2005;21:4842.
[40] Tcholakova S, Denkov ND, Borwankar R, Campbell B. Van der Waals interaction between two truncated spheres covered by a uniform layer (deformed drops, vesicles, bubbles). Langmuir 2001;17:2357.
[41] Roth CM, Neal BL, Lenhoff AM. Van der Waals interactions involving proteins. Biophys J 1996;70:977.
[42] Dimitrova TD, Leal-Calderon F, Gurkov TD, Campbell B. Disjoining pressure vs. thickness isotherms of thin emulsion films stabilized by proteins. Langmuir 2001;17:8069.
[43] Dimitrova TD, Leal-Calderon F. Rheological properties of highly concentrated protein-stabilized emulsions. Adv Colloid Interface Sci 2004;108–109:49.
[44] Denkov ND, Tcholakova S, Ivanov IB, Campbell B. Methods for evaluation of emulsion stability at a single drop level, Paper included in the Third World Congress on Emulsions, Lyon 2002, Paper No. 198.
[45] Tcholakova S, Denkov ND, Ivanov IB, Campbell B. Coalescence in β-lactoglobulin-stabilized emulsions: effects of protein adsorption and drop size. Langmuir 2002;18:8960.
[46] Tcholakova S, Marinov R, Denkov ND, Ivanov IB. Evaluation of short-term and long-term stability of emulsions by centrifugation and NMR. Bulg J Phys 2004;31:96.
[47] Tcholakova S, Denkov ND, Sidzhakova D, Ivanov IB, Campbell B. Effects of thermal treatment ionic strength, and pH on the short-term and long-term coalescence stability of β-lactoglobulin emulsions. Langmuir in press.
[48] The experiments described in Sections 6.1, 7.1, 9.1 were performed with a different batch of BLG. At equivalent conditions, the coalescence stability of emulsions prepared with this batch was somewhat lower than the stability of the emulsions described in the other sections (no significant difference in any other emulsion characteristic was detected). The most probable explanation is a different ratio of variants A and B in the two BLG batches used [49]. Therefore, it is impossible to make direct quantitative comparison of the data for the coalescence stability between Sections 6.1, 7.1, 9.1 and the other sections. However, comparative experiments showed that all trends in the coalescence stability, described in the current review, are well reproduced with all of the BLG batches used.
[49] Euston SR, Hirst RL, Hill JP. The emulsifying properties of b-lactoglobulin genetic variants A, B and C. Colloids Surf B Biointerfaces 1999;12:193.
[50] Gaonkar AG, Borwankar RP. Competitive adsorption of monoglycerides and lecithin at the vegetable oil–water interface. Colloids Surf 1991;59: 331.
[51] Sather O. Video-enhanced microscopy investigation of emulsion droplets and size distributions. In: Sjöblom J, editor. Encyclopedic Handbook of Emulsion Technology. New York: Marcel Decker; 2001. p. 349. Chapter 15.
[52] Jokela P, Fletcher P, Aveyard R, Lu J. The use of computerized microscopic image analysis to determine emulsion droplet size distributions. J Colloid Interface Sci 1990;113:417.
[53] Denkova PS, Tcholakova S, Denkov ND, Danov KD, Campbell B, Shawl C, et al. Evaluation of the precision of drop-size determination in oil/water emulsions by low resolution NMR spectroscopy. Langmuir 2004;20:11402.
[54] Bradford M. A rapid and sensitive method for the quantitation of microgram quantities of protein utilizing the principle of protein–dye binding. Anal Biochem 1976;72:248.
[55] Hadjiiski A, Tcholakova S, Denkov ND, Durbut P, Broze G, Mehreteab A. Effect of oily additives on foamability and foam stability: 2. Entry barriers. Langmuir 2001;17:7011.
[56] Hadjiiski A, Tcholakova S, Ivanov IB, Gurkov TD, Leonard E. Gentle film trapping technique with application to drop entry measurements. Langmuir 2002;18:127.
[57] Ivanov IB, Basheva E, Gurkov TD, Hadjiiski A, Arnaudov L, Vassileva N, et al. Stability of oil-in-water emulsions containing protein. In: Dickinson E, Miller R, editors. Food Colloids 2000, Fundamentals of Formulation. Cambridge: Royal Society of Chemistry; 2001. p. 73.
[58] Vold RD, Groot RC. An ultracentrifugal method for the quantitative determination of emulsion stability. J Phys Chem 1962;66:1969.
[59] Vold RD, Groot RC. The effect of electrolytes on the ultracentrifugal stability of emulsions. J Colloid Interface Sci 1964;19:384.
[60] Mittal KL, Vold RD. Effect of the initial concentration of emulsifying agents on the ultracentrifugal stability of oil-in-water emulsions. J Am Oil Chem Soc 1972;49:527.
[61] Smith AL, Mitchell DP. The centrifuge technique in the study of emulsion stability. In: Smith AL, editor. Theory and Practice of Emulsion Technology. New York: Academic Press; 1976. p. 61–74.
[62] Vold RD, Mittal KL, Hahn AU. Ultracentrifugal stability of emulsions. In: Matijevic E, editor. Surface and Colloid Science, vol. 10. New York: Plenum Press; 1978.
[63] Taisne L, Walstra P, Cabane B. Transfer of oil between emulsion droplets. J Colloid Interface Sci 1996;184:378.
[64] van Aken GA, Zoet FD. Coalescence in highly concentrated emulsions. Langmuir 2000;16:7131.
[65] Kolmogoroff AN. Drop breakage in turbulent flow. Compt Rend Acad Sci URSS 1949;66:825 [in Russian].
[66] Hinze JO. Fundamentals of the hydrodynamic mechanism of splitting in dispersion processes. AIChE J 1955;3:289.

[67] Batchelor GK. The Theory of Homogeneous Turbulence. Cambridge: Cambridge University Press; 1953.
[68] Coulaloglou CA, Tavlarides LL. Description of interaction processes in agitated liquid–liquid dispersions. Chem Eng Sci 1977;32:1289.
[69] Tsouris C, Tavlarides LL. Breakage and coalescence models for drops in turbulent dispersions. AIChE J 1994;40:395.
[70] Sprow FB. Distribution of drop sizes produced in turbulent liquid–liquid dispersion. Chem Eng Sci 1967;22:435.
[71] Teppner R, Steiner H, Brenn G, Vankova N, Tcholakova S, Denkov N. Numerical simulation and experimental study of emulsification in a narrow-gap homogenizer, Chem Eng Sci in press.
[72] Shreekumar B, Kumar R, Gandhi KS. Breakage of a drop of inviscid fluid due to a pressure fluctuation at its surface. J Fluid Mech 1996;328: 1.
[73] Davies JT. Drop sizes of emulsions related to turbulent energy dissipation rates. Chem Eng Sci 1985;40:839.
[74] Calabrese RV, Chang TPK, Dang PT. Drop breakage in turbulent stirred-tank contractors. Part I: Effect of dispersed-phase viscosity. AIChE J 1986;32:657.
[75] Wang CY, Calabrese RV. Drop breakage in turbulent stirred-tank contractors. Part II: Relative influence of viscosity and interfacial tension. AIChE J 1986;32:667.
[76] Calabrese RV, Wang CY, Bryner NP. Drop breakage in turbulent stirred-tank contractors. Part III: Correlations for mean size and drop size distribution. AIChE J 1986;32:677.
[77] Lagisetty JS, Das PK, Kumar R, Gandhi KS. Breakage of viscous and non-Newtonian drops in stirred dispersions. Chem Eng Sci 1986;41:65.
[78] Vankova N, Tcholakova S, Denkov ND, Ivanov IB, Danner T. Emulsification in turbulent flow: Part 2. Breakage rate constants. Colloids Surf (submitted for publication).
[79] Arditty S, Whitby CP, Binks BP, Schmitt V, Leal-Calderon F. Some general features of limited coalescence in solid-stabilized emulsions. Eur Phys J E 2003;11:273.
[80] Giermanska-Kahn J, Laine V, Arditty S, Schmitt V, Leal-Calderon F. Particle-stabilized emulsions comprised of solid droplets. Langmuir 2005;21: 4316.
[81] Bibette J, Morse DC, Witten TA, Weitz DA. Stability criteria for emulsions. Phys Rev Lett 1992;69:2439.
[82] Bibette J, Leal-Calderon F, Poulin P. Emulsions: basic principles. Rep Prog Phys 1999;62:969.
[83] van Aken GA, van Vliet T. Mechanism of coalescence in highly concentrated protein-stabilized emulsions. In: Dickinson E, Miller R, editors. Food Colloids 2000, Fundamentals of Formulation. Cambridge: Royal Society of Chemistry; 2001. p. 125.
[84] Das KP, Kinsella JE. Droplet size and coalescence stability of whey protein stabilized milkfat peanut oil emulsions. J Food Sci 1993;58:439.
[85] Mohan S, Narsimhan G. Coalescence of protein-stabilized emulsions in a high-pressure homogenizer. J Colloid Interface Sci 1997;192:1.
[86] Narsimhan G, Goel P. Drop coalescence during emulsion formation in a high-pressure homogenizer for tetradecane-in-water emulsion stabilized by sodium dodecyl sulfate. J Colloid Interface Sci 2001;238:420.
[87] Das KP, Kinsella JE. pH dependent emulsifying properties of b-lactoglobulin. J Dispers Sci Technol 1989;10:77.
[88] Khristov Khr, Exerowa D, Minkov G. Critical capillary pressure for destruction of single foam films and foam: effect of foam film size. Colloids Surf A Physicochem Eng Asp 2002;210:159.
[89] Denkov ND. Mechanisms of foam destruction by oil-based antifoams. Langmuir 2004;20:9463.
[90] Princen HM. Pressure/volume/surface area relationships in foams and highly concentrated emulsions: role of volume fraction. Langmuir 1988;4: 164.
[91] Princen HM. The structure, mechanics, and rheology of concentrated emulsions and fluid foams. In: Söblom J, editor. Encyclopedic Handbook of Emulsion Technology. New York: Marcel Dekker; 2001. Chapter 11.
[92] Princen HM. Osmotic pressure of foams and highly concentrated emulsions. 1. Theoretical consideration. Langmuir 1986;2:519.
[93] Princen HM. Osmotic pressure of foams and highly concentrated emulsions. 2. Determination from the variation in volume fraction with height in an equilibrated column. Langmuir 1987;3:36.
[94] Mason TG. Rheology of monodisperse emulsions, Ph.D. Thesis, Department of Physics, Princeton University, 1995.
[95] Cox SJ, Weaire D, Hutzler S, Murphy J, Phelan R, Verbist G. Applications and generalizations of the foam drainage equation. Proc R Soc Lond A 2000;456:2441.
[96] Cornec M, Cho D, Narsimhan G. Adsorption dynamics of a-Lactalbumin and b-Lactoglobulin at air–water interfaces. J Colloid Interface Sci 1999;214:129.
[97] Lu JR, Su TJ, Thomas RK. Structural conformation of bovine serum albumin layers at the air–water interface studied by neutron reflection. J Colloid Interface Sci 1999;213:426.
[98] Gauthier F, Bouhallab S, Renault A. Modification of bovine b-lactoglobulin by glycation in a powdered state or in aqueous solution: adsorption at air–water interface. Colloids Surf B Biointerfaces 2001;21:37.
[99] Bylaite E, Nylander T, Vensutonis R, Jonson B. Emulsification of caraway essential oil in water by lecithin and b-lactoglobulin: emulsion stability and properties of the formed oil–aqueous interface. Colloids Surf B Biointerfaces 2001;20:327.
[100] Boerboom FJG, de Goot-Mostert AEA, Prins A, van Vliet T. Bulk and surface rheological behaviour of aqueous milk protein solutions. A comparison. Neth Milk Dairy J 1996;50:183.
[101] Miller R, Fainerman VB, Makievski AV, Grigoriev DO, Wilde P, Krägel J. Dynamic properties of protein+surfactant mixtures at the air–liquid interface. In: Dickinson E, Rodriguez Patino JM, editors. Food Emulsions and Foams: Interfaces, Interactions and Stability. Cambridge: Royal Society of Chemistry; 1999. p. 207.
[102] Gurkov TD, Russev SC, Danov KD, Ivanov IB, Campbell B. Monolayers of globular proteins on air/water interface: applicability of the Volmer equation of state. Langmuir 2003;19:7362.
[103] Svitova TF, Wetherbee MJ, Radke CJ. Dynamics of surfactant sorption at the air/water interface: continuous-flow tensiometry. J Colloid Interface Sci 2003;261:170.
[104] Cascao Pereira LG, Johansson Ch, Radke CJ, Blanch H. Surface forces and drainage kinetics of protein-stabilized aqueous films. Langmuir 2003;19:7503.
[105] Israelachvili JN. Intermolecular and Surface Forces. 2nd ed. New York: Academic Press; 1992. Chapters 11–14.
[106] Derjaguin BV, Churaev NV, Muller VM. Surface Forces. New York: Plenum Press; 1987.
[107] Kralchevsky PA, Danov KD, Denkov ND. Chemical physics of colloid systems and interfaces. In: Birdi KS, editor. Handbook of Surface and Colloid Chemistry. Second Expanded and Updated Edition. Boca Raton, FL: CRC Press; 2002. Chapter 5.
[108] Dolan AK, Edwards SF. Theory of the stabilization of colloids by adsorbed polymer. Proc R Soc Lond 1974;A337:509.
[109] de Gennes PG. Polymers at an interface: a simplified view. Adv Colloid Interface Sci 1987;27:189.
[110] Semenov N, Joanny J-F, Johner A, Bonet-Avalos J. Interaction between two adsorbing plates: the effect of polymer chain ends. Macromolecules 1997;30:1479.
[111] Dimitrova TD, Vassileva N, Campbell B. (in preparation).
[112] Damodaran S, Anand K. Sulfhydryl–disulfide interchange-induced interparticle protein polymerization in whey protein-stabilized emulsions and its relation to emulsion stability. J Agric Food Chem 1997;45:3813.
[113] Fang Y, Dalgleish DG. Conformation of b-lactoglobulin studied by FTIR: effect of pH, temperature, and adsorption to the oil–water interface. J Colloid Interface Sci 1997;196:292.
[114] Sliwinski EL, Roubos PJ, Zoet FD, van Boekel MAJS, Wouters JTM. Effects of heat on physicochemical properties of whey protein-stabilized emulsions. Colloids Surf B Biointerfaces 2003;31:231.
[115] Sliwinski EL, Lavrijsen BWM, Vollenbroek JM, van der Stege HJ, van Boekel MAJS, Wouters JTM. Effects of spray drying on physicochemical properties of milk protein-stabilised emulsions. Colloids Surf B Biointerfaces 2003;31:219.
[116] Sourdet S, Relkin P, Cesar B. Effects of milk protein type and pre-heating on physical stability of whipped and frozen emulsions. Colloids Surf B Biointerfaces 2003;31:55.

[117] Monahan FJ, McClements DJ, German JB. Disulfide-mediated polymerization reactions and physical properties of heated WPI-stabilized emulsions. J Food Sci 1996;61:504.
[118] Murray BS. Interfacial rheology of mixed food protein and surfactant adsorption layers with respect to emulsion and foam stability. In: Mobius D, Miller R, editors. Proteins at Liquid Interfaces. Amsterdam: Elsevier; 1998.
[119] Hoffmann M, Sala G, Olieman G, Kruif KG. Molecular mass distribution of heat-induced b-lactoglobulin aggregates. J Agric Food Chem 1997;45: 2949.
[120] Pace NC, Tanford C. Thermodynamics of the unfolding of β-lactoglobulin A in aqueous urea solutions between 5 and 55 °C. Biochemistry 1968;7: 198.
[121] Das KP, Kinsella JE. Effect of heat denaturation on the adsorption of b-lactoglobulin at oil/water interface and on coalescence stability of emulsions. J Colloid Interface Sci 1990;139:551.
[122] Boye JI, Ma CY, Ismail A, Harwalkar VR, Kalab M. Molecular and microstructural studies of thermal denaturation and gelation of b-lactoglobulins A and B. J Agric Food Chem 1997;45:1608.
[123] Dong A, Huang P, Caughey WS. Protein secondary structures in water from second-derivative amide I infrared spectra. Biochemistry 1990;29: 3303.
[124] Qi X, Holt C, Mcnulty D, Clarke DT, Brownlow S, Jones G. Effect of temperature on the secondary structure of b-lactoglobulin at pH 6.7, as determined by CD and IR spectroscopy: a test of the molten globule hypothesis. Biochem J 1997;324:341.
[125] Velikov KP, Durst F, Velev OD. Direct observation of the dynamics of latex particles confined inside thinning water–air films. Langmuir 1998;14: 1148.
[126] Horozov TS, Aveyard R, Clint JH, Neumann B. Particle zips: vertical emulsion films with particle monolayers at their surfaces. Langmuir 2005;21:2330.
[127] Denkov ND, Velev OD, Kralchevsky PA, Ivanov IB, Yoshimura H, Nagayama K. Mechanism of formation of two-dimensional crystals from latex particles on substrates. Langmuir 1992;8:3183.
[128] Lazarov GS, Denkov ND, Velev OD, Kralchevsky PA, Nagayama K. Formation of 2D-structures on fluorinated-oil substratum. J Chem Soc Faraday Trans 1994;90:2077.
[129] Danov KD, Pouligny B, Kralchevsky PA. Capillary forces between colloidal particles confined in a liquid film: the finite-meniscus problem. Langmuir 2001;17:6599.
[130] van Aken GA, van Vliet T. Flow-induced coalescence in protein-stabilized highly concentrated emulsions: role of shear-resisting connections between the droplets. Langmuir 2002;18:7364.
[131] Hotrum NE, Cohen Stuart MA, van Vliet T, van Aken GA. Flow and fracture phenomena in adsorbed protein layers at the air/water interface in connection with spreading oil droplets. Langmuir 2003;19:10210.
[132] van Aken GA. Flow-induced coalescence in protein-stabilized highly concentrated emulsions. Langmuir 2002;18:2549.
[133] Kim HJ, Decker EA, McClements DJ. Effect of cosolvents on thermal stability of globular protein-stabilized emulsions, Paper included in the Proceedings of the Third World Congress on Emulsions, Lyon 2002, Paper No. 035
[134] Kim H-J, Decker EA, McClements DJ. Impact of protein surface denaturation on droplet flocculation in hexadecane oil-in-water emulsions stabilized by beta-lactoglobulin. J Agric Food Chem 2002;50:7131.
[135] Kim H-J, Decker EA, McClements DJ. Role of postadsorption conformation changes of beta-lactoglobulin on its ability to stabilize oil droplets against flocculation during heating at neutral pH. Langmuir 2002;18:7577.
[136] Kim H-J, Decker EA, McClements DJ. Influence of sucrose on droplet flocculation in hexadecane oil-in-water emulsions stabilized by b-lactoglobulin. J Agric Food Chem 2003;51:766.
[137] Gu YS, Decker EA, McClements DJ. Influence of pH and carrageenan type on properties of b-lactoglobulin stabilized oil-in-water emulsions. Food Hydrocol 2005;19:83.
[138] Kim H-J, Decker EA, McClements DJ. Influence of free protein on flocculation stability of β-lactoglobulin stabilized oil-in-water emulsions at neutral pH and ambient temperature. Langmuir 2004;20:10394.
[139] Kim H-J, Decker EA, McClements DJ. Influence of protein concentration and order of addition on thermal stability of β-lactoglobulin stabilized n-hexadecane oil-in-water emulsions at neutral pH. Langmuir 2005;21:134.
[140] Kim H-J, Decker EA, McClements DJ. Comparison of droplet flocculation in hexadecane oil-in-water emulsions stabilized by β-lactoglobulin at pH 3 and 7. Langmuir 2004;20:5753.
[141] Smith PK, Krohn RI, Hermanson GT, Mallia AK, Gartner FH, Provenzano MD, et al. Measurement of protein using bicinchoninic acid. Anal Biochem 1985;150:76.